

Modeling carbon dynamics in vegetation and soil under the impact of soil erosion and deposition

Shuguang Liu and Norman Bliss

U.S. Geological Survey, Earth Resources Observation Systems Data Center, SAIC, Sioux Falls, South Dakota, USA

Eric Sundquist

U.S. Geological Survey, Woods Hole, Massachusetts, USA

Thomas G. Huntington

U.S. Geological Survey, Augusta, Maine, USA

Received 6 November 2002; revised 7 April 2003; accepted 23 April 2003; published 26 June 2003.

[1] Soil erosion and deposition may play important roles in balancing the global atmospheric carbon budget through their impacts on the net exchange of carbon between terrestrial ecosystems and the atmosphere. Few models and studies have been designed to assess these impacts. In this study, we developed a general ecosystem model, Erosion-Deposition-Carbon-Model (EDCM), to dynamically simulate the influences of rainfall-induced soil erosion and deposition on soil organic carbon (SOC) dynamics in soil profiles. EDCM was applied to several landscape positions in the Nelson Farm watershed in Mississippi, including ridge top (without erosion or deposition), eroding hillslopes, and depositional sites that had been converted from native forests to croplands in 1870. Erosion reduced the SOC storage at the eroding sites and deposition increased the SOC storage at the depositional areas compared with the site without erosion or deposition. Results indicated that soils were consistently carbon sources to the atmosphere at all landscape positions from 1870 to 1950, with lowest source strength at the eroding sites (13 to 24 $\text{gC m}^{-2} \text{yr}^{-1}$), intermediate at the ridge top (34 $\text{gC m}^{-2} \text{yr}^{-1}$), and highest at the depositional sites (42 to 49 $\text{gC m}^{-2} \text{yr}^{-1}$). During this period, erosion reduced carbon emissions via dynamically replacing surface soil with subsurface soil that had lower SOC contents (quantity change) and higher passive SOC fractions (quality change). Soils at all landscape positions became carbon sinks from 1950 to 1997 due to changes in management practices (e.g., intensification of fertilization and crop genetic improvement). The sink strengths were highest at the eroding sites (42 to 44 $\text{gC m}^{-2} \text{yr}^{-1}$), intermediate at the ridge top (35 $\text{gC m}^{-2} \text{yr}^{-1}$), and lowest at the depositional sites (26 to 29 $\text{gC m}^{-2} \text{yr}^{-1}$). During this period, erosion enhanced carbon uptake at the eroding sites by continuously taking away a fraction of SOC that can be replenished with enhanced plant residue input. Overall, soil erosion and deposition reduced CO_2 emissions from the soil into the atmosphere by exposing low carbon-bearing soil at eroding sites and by burying SOC at depositional sites. The results suggest that failing to account for the impact of soil erosion and deposition may potentially contribute to an overestimation of both the total historical carbon released from soils owing to land use change and the contemporary carbon sequestration rates at the eroding sites. *INDEX TERMS*: 1615 Global Change: Biogeochemical processes (4805); 1630 Global Change: Impact phenomena; 1815 Hydrology: Erosion and sedimentation; 3210 Mathematical Geophysics: Modeling; *KEYWORDS*: carbon dynamics, model simulations, EDCM model, erosion, deposition

Citation: Liu, S., N. Bliss, E. Sundquist, and T. G. Huntington, Modeling carbon dynamics in vegetation and soil under the impact of soil erosion and deposition, *Global Biogeochem. Cycles*, 17(2), 1074, doi:10.1029/2002GB002010, 2003.

1. Introduction

[2] Conversion of lands from a native state to an agricultural use usually leads to a 20–40% reduction in soil organic

carbon (SOC) storage [Donigian *et al.*, 1994; Paul *et al.*, 1997; Buyanovsky and Wagner, 1998a; Harden *et al.*, 1999]. It is often implicitly assumed that the SOC that is lost is released to the atmosphere [DeFries *et al.*, 1999; Houghton *et al.*, 1999; Hurtt *et al.*, 2002]. In fact, in addition to the atmospheric pathway, erosion can also contribute to SOC

loss from uplands [Slater and Carleton, 1938; Webber, 1964; Tiessen et al., 1982; Geng and Coote, 1991; Cihacek and Swan, 1994; Lal, 1995; Harden et al., 1999]. Some of the eroded soil, carbon, and nutrients are redistributed across the landscape, and some are transported and deposited to waterlogged environments, such as reservoirs, lakes, wetlands and oceans [Lal, 1995; Stallard, 1998; Smith et al., 2001]. Stallard [1998] estimated that a significant portion of the missing sink of atmospheric CO₂ (1.2–2.0 Pg C yr⁻¹) [Schimel et al., 1995, 2001] could be explained by the SOC eroded and redeposited annually if the redeposited SOC is replaced by sequestering new SOC from the atmosphere at the eroding sites. Stallard [1998] analyzed a range of scenarios for global redeposition of eroded SOC in both waterlogged and upland environments. Schimel et al. [1985] hypothesized that depositional upland sites are sinks for C because of the burial and reduced decomposition caused by physical protection of organic matter. Because erosion concentrates clay particles, organic matter, and soluble nutrients at depositional sites, the formation of soil aggregates at these areas could be enhanced and therefore lead to increased physical and chemical protection of SOC and reduced SOC turnover. Whether eroded SOC is translocated across uplands or deposited in waterlogged environments, depositional areas are therefore likely to accumulate carbon. As suggested by Stallard [1998], the extent to which erosion and deposition lead to an atmospheric C sink depends on how much of the depositional accumulation is replaced by newly produced SOC in the eroding uplands. However, this analysis is difficult to verify because the formation of new SOC is an ongoing process in most landscape settings, whether they are undisturbed or subject to erosion or deposition. The fate of the eroded SOC, the impact of soil erosion on the SOC remaining at the eroding sites, and the impact of deposition on the SOC buried at the depositional sites are all important pieces of the whole puzzle. Owing to the difficulty of deploying field experiments for direct assessment, it is important to develop mechanistic models to improve our understanding of the overall impact of the soil erosion and deposition on SOC.

[3] In previous publications, three kinds of models have been used to assess the impact of soil erosion on SOC dynamics at the eroding sites [Bouwman, 1989; Vermeulen et al., 1993; Harden et al., 1999], and no counterpart models have been available for depositional sites. The first group includes models that are designed to investigate the impact of soil erosion on soil organic matter [e.g., Voroney et al., 1981; Bouwman, 1989]. In these models, some ecosystem properties, such as net primary production and the level of plant residue input into the soil, were prescribed as constants and did not vary over time. Thus the interactions and feedback between erosion and primary production could not be considered.

[4] A second modeling approach is represented by the Erosion Productivity Impact Calculator (EPIC) [Williams, 1995], in which the primary emphasis is to evaluate the impact of soil erosion on the productivity of crops rather than SOC dynamics. The capability of this model to predict SOC dynamics has not been tested extensively. Nevertheless, the EPIC model has been used to simulate the impact

of soil erosion on SOC at 100 randomly selected plots in the U.S. corn belt under various management and climatic scenarios [Lee et al., 1993, 1996].

[5] The third modeling approach relies on biogeochemical models that simulate the dynamics of carbon and nutrients in vegetation and soil. So far, only two models are reported to have incorporated erosion processes into biogeochemical cycles: CENTURY [Harden et al., 1999] and Soil Change Under AgroForestry (SCUAF) [Vermeulen et al., 1993]. SCUAF is specifically designed for agroforestry systems, and it is still under development. The CENTURY model has been tested widely against field measurements of primary production, SOC, and nitrogen dynamics under various conditions [Parton et al., 1987, 1993; Schimel et al., 1994; VEMAP Members, 1995; Smith et al., 1997]. Unfortunately, the impact of soil erosion was not included in most tests of the CENTURY model. If the impact of erosion and deposition is not considered, the net emissions of carbon from agricultural activities into the atmosphere may be overestimated.

[6] In this study, we present an ecosystem model that is capable of simulating the impacts of both soil erosion and deposition on SOC dynamics. We then apply the model to an examination of the historical SOC trajectories and the apparent SOC loss under various erosion, deposition, and management scenarios at a field site. Finally, we examine uncertainties in our calculations by analysis of model sensitivity to various input variables.

2. Sites and Field Measurements

[7] The study site was at the Nelson Farm, located in Tate County, Mississippi, with latitude 34°33'50" and longitude 89°57'30". The Nelson Farm site is a small hydrologically monitored headwater watershed with an area of 2.09 ha. Soils, derived from Peoria Loess parent material, were described as eroded Memphis silt loam (Typic Hapludalf) on the broad ridges and severely eroded Grenada silt loam (Glossic Fragiudalfs) on the hillslopes [Huddleston, 1967]. Annual precipitation is about 1340 mm, and annual average daily maximum and minimum air temperatures are 23.9°C and 10.6°C, respectively.

[8] Our study utilizes the data compiled for Nelson Farm during previous work by researchers from the U.S. Geological Survey [Huntington et al., 1998; Sharpe et al., 1998; Harden et al., 1999]. Nelson Farm was converted from forests to agriculture around 1870 and used primarily for cotton production until about 1950 (Table 1). Historical management information, including crops cultivated, types of tillage, harvest, and fertilizer application, are listed in Table 1, which is adapted largely from Sharpe et al. [1998] and Harden et al. [1999]. The SOC contents at various slope positions (upper or ridge, middle, and lower) were measured in 1996 [Harden et al., 1999]. In this study, the sites located at the ridge top were considered as the control sites, without erosion or deposition. However, we recognize that the ridge top sites might have experienced soil erosion as well due to tillage translocation [Harden et al., 1999]. The sites at the middle slope were considered as eroding sites, and the ones at the lower slope were depositional sites.

Table 1. Erosion Rates and Land Use History on the Nelson Farm (Adapted From *Sharpe et al.* [1998] and *Harden et al.* [1999])

From	To	Duration, years	Erosion, kg soil m ⁻² yr ⁻¹		Species ^a	Cultivation ^b	Fertilization ^c	Harvest ^d
			Minimum	Maximum				
1870	1870	1	0.003	0.02	CWT			
1871	1871	1	0.003	0.02	GGCP	AT-7		
1872	1882	11	0.07	0.17	GGCP			
1883	1929	47	3.8	12.3	COT	AT-7		GS
1930	1936	7	3.8	10.67	COT	AT-7	N3, PS2, N3, PS2, N3, PS2	GS
1937	1945	9	1.11	4.4	COT	AT-7	N3, PS2, N3, PS2	GS
1946	1946	1	8.59	8.59	COT	AT-7	N3, PS2, N3, PS2	GS
1947	1950	4	1.11	4.4	COT	AT-7	PS2, N3, PS2, N3	GS
1951	1953	3	0.85	0.85	SORG	P		H
1954	1967	14	1.95	4.4	SYBN	P	PS2, A90, A90	G
1968	1980	13	1.51	2.15	C-HI	P, ROW, ROW	MAX, MAX, MAX	GS
1981	1982	1	0.40	0.76	W3	P, P	PS2, N3	G
1982	1983	1	0.24	0.24	W3	P	N3	G
1983	1984	1	0.24	0.24	W3	P		G
1984	1986	3	0.24	0.24	G3			G
1987	1987	1	0.24	0.24	W3	H, C, P, R		G
1988	1988	1	1.74	1.74	SYBN	P, ROW, C	PS2	G
1989	1989	1	4.4	4.4	SYBN	P, H, C, C	PS2	G
1990	1990	1	0.97	0.97	SYBN	H, P, H, P, H, C, C	PS2	G
1991	1991	1	3.28	3.28	SYBN	H, P, S, C	PS2	G
1992	1992	1	1.84	1.84	SYBN	H, P, P, S, H, C	PS2	G
1993	1993	1	0.22	0.22	SYBN	P, P, C	A90, A90, A90	G
1994	1994	1	2.14	2.14	SYBN	P, P, P, H, C	A90, A90, A90	G
1995	1997	3	0.64	0.64	SYBN	P, P, ROW, C	A90, A90, A90	G

^aSpecies: CWT, Coweeta broadleaved forest; GGCP, pasture with 3/4 temperate grass; COT, cotton; SORG, sorghum; SYBN, soybeans; C-HI, corn with the highest yield; W3, wheat with high harvest index; G3, grass mixed with 50% warm and 50% cool.

^bCultivation: AT-7, animal-tillage; P, plowing; ROW, row cultivator; C, cultivator; H, herbicide; S, sweep.

^cFertilization: N3, 30 kgN ha⁻¹; PS2, superphosphate 250 kg ha⁻¹; A90, automatic fertilization to maintain production at 90% of the maximum; MAX, automatic fertilization to maintain the maximum production.

^dHarvest: GS, grain with 50% removal of the aboveground nongrain biomass; H, hay; G, grain.

[9] *Harden et al.* [1999] also measured soil carbon profiles at several nearby forested sites, providing references to the possible SOC conditions of the forests around 1870, just prior to cutting and conversion to agriculture. The main forest sites (i.e., Goodwin Creek) were located in a mixed hardwood forest with an area of about 20 acres and an age of at least 80 years. The aboveground net primary productivity (AGNPP) was 335 g C m⁻² yr⁻¹ at the Goodwin Creek site. SOC contents and bulk density of soils at various depths were given by *Harden et al.* [1999].

3. Metrics for Impact Assessment

3.1. Atmospheric C Sources/Sinks Under Erosion and Deposition: Φ

[10] For sites with erosion or deposition, the net change of SOC in the whole profile can be expressed by the following mass conservation equation:

$$\frac{dC}{dt} = C_{litter} - kC + C_x, \quad (1)$$

where k is the decomposition coefficient of SOC (C), C_{litter} is C input from litter, and C_x is the C eroded (negative) or deposited (positive). Therefore the net C exchange between the soil and atmosphere (Φ , or the source/sink strength of atmospheric carbon) can be calculated as

$$\Phi = \frac{dC}{dt} - C_x. \quad (2)$$

When Φ is positive, the soil is acting as a sink, and vice versa. Equations (1) and (2) can be applied to either terrestrial or aquatic ecosystems.

3.2. Impact of Soil Erosion and Deposition on SOC Stock: ψ

[11] Impact of soil erosion or deposition (ψ) on SOC stock is defined as the difference between the SOC stock at an erosional or depositional site (C_t) and that at a control site without erosion or deposition ($C_{0,t}$) at time t ,

$$\psi = C_t - C_{0,t}. \quad (3)$$

It is assumed in equation (3) that the initial conditions at time 0 for the control site and the erosional or depositional site are identical and the only difference between the sites is erosion or deposition. In a relative term, ψ becomes

$$\psi_{\%} = \frac{C_t - C_{0,t}}{C_0} \times 100\%, \quad (4)$$

where C_0 is the initial SOC stock.

3.3. Impact of Soil Erosion and Deposition on SOC Sink/Source: Ω

[12] In a manner similar to equation (3), the impact of erosion or deposition on atmospheric C sink or source (Ω) can be quantified as follows:

$$\Omega = \Phi_t - \Phi_{0,t}, \quad (5)$$

where Φ_t and $\Phi_{0,t}$ are the carbon source/sink strength at the erosional or depositional site and the control site, respectively, at time t as defined by equation (2). This approach is site specific and cannot be applied directly to calculation of aggregate effects among eroding and depositional sites within a landscape, where it will be necessary to account for the relative areas of erosion and deposition, and for the rate of decomposition of SOC during transport.

4. Structure and Major Characteristics of EDCM

[13] In this section, we introduce the major characteristics of the newly developed model Erosion-Deposition-Carbon-Model (EDCM), including its features derived from the well-established CENTURY model, and methods and algorithms for tracking the evolution of soil characteristics of soil profiles under the influence of soil erosion or deposition. Other characteristics of EDCM (e.g., the algorithms for calculating net primary production considering historical changes in crop genetics and harvesting practices, the methods for predicting soil temperature profiles, and the simulation of SOC decomposition in deep layers) are given in Appendix A.

4.1. EDCM and Its Relationship With CENTURY IV

[14] EDCM is an ecosystem model based on the well-established ecosystem model CENTURY (CENTURY refers to CENTURY version IV in this paper unless explicitly specified otherwise) [Parton *et al.*, 1987, 1993]. EDCM was developed to account for the SOC dynamics in the whole soil profile and to be capable of considering the impact of soil erosion and deposition. We used CENTURY as a basis for developing EDCM because CENTURY has been tested widely around the world at various spatial scales [Parton *et al.*, 1993; Schimel *et al.*, 1994; VEMAP Members, 1995], and the algorithms for the prediction of SOC dynamics are well tested. These established algorithms form the basis of several other biogeochemical models, such as CASA [Potter *et al.*, 1993], InTEC [Chen *et al.*, 2000], and TRIPLEX [Peng *et al.*, 2002]. CENTURY has a one-soil-layer structure for carbon and nutrients. In contrast, EDCM adopts a multisoil-layer structure to account for the stratification of the soil profile and SOC in each soil layer. EDCM dynamically keeps track of the evolution of the soil profile and carbon storage as influenced by soil erosion and deposition.

[15] CENTURY simulates carbon and nutrient dynamics in the top 20-cm soil layer, which is set as a constant in the model. This fixed top layer approach is appropriate for many applications because most of the soil biological activity takes place in this layer. However, it may severely limit the model's capability to simulate the impacts of soil erosion and deposition on soil profile properties such as SOC. Some important processes, such as the impacts of soil erosion and deposition on the SOC below the top layer, cannot be realistically simulated with the existing model structure.

[16] For example, to adapt the CENTURY model to accommodate the impact of soil erosion and deposition on SOC, Harden *et al.* [1999] retained the basic one layer structure of CENTURY for biogeochemical processes, but added two external C pools. The two external C pools,

referred to here as the "subsoil" and "eroded" pools, were designated for keeping account of the amount of carbon below the top layer and the amount of carbon that is eroded, respectively. In this approach, the "subsoil" SOC, once initialized, can only be changed by adjustment to conserve mass during soil erosion. In this adjustment, a portion of the subsoil is transferred to the top layer in order to keep the thickness of the top layer constant during erosion. No algorithms are implemented in CENTURY, or in the adaptation of Harden *et al.*, to consider the impacts of biophysical processes, such as decomposition and root growth and senescence on the SOC amount contained in the "subsoil" C pool. This static accounting approach cannot accommodate intrinsic changes caused by the alterations of land cover types, which may have different rooting properties, and the subsoil changes in susceptibility to decomposition, which may be very sensitive to changes of soil depth.

[17] The fate of the carbon in the "eroded" C pools of Harden *et al.* [1999] was evaluated using a spreadsheet model and arbitrary decomposition coefficients. CENTURY does not have the capability of simulating SOC dynamics in depositional environments. Although the approach of Harden *et al.* provided a qualitative analytical structure to evaluate the possible fate of eroded carbon with minimal modification of the CENTURY model, the calculations relating to the "subsoil" and "eroded" C pools cannot be constrained by field data or used to evaluate SOC dynamics at the depositional sites.

[18] CENTURY has limited capability for predicting the impact of soil erosion and deposition on SOC and is not capable of simulating SOC dynamics in deep soil layers. However, CENTURY has a set of widely tested algorithms for the simulation of SOC and nutrient dynamics in the top 20-cm layer. The EDCM model retains this set of algorithms for the top layer and uses them as the primary basis for the simulation of SOC dynamics in deep soil layers. This treatment retains the proven applicability of CENTURY model for the topsoil layer and provides consistency between the top layer and the deeper layers in EDCM simulations. This inheritance in modeling approaches not only makes EDCM as robust as CENTURY in simulating ecosystem dynamics but also adds another dimension for simulating the impacts of soil erosion and deposition processes on SOC.

4.2. Multisoil-Layer Model Structure

[19] To simulate the dynamics of SOC under nonequilibrium conditions, models with a multisoil-layer structure are necessary [Bouwman, 1989; Sharpley and Williams, 1990]. Under the influence of soil erosion or deposition, characteristics of the soil profile and SOC in all the soil layers must change dynamically. If the thickness of the top layer is fixed, its SOC content must experience a dynamic replacement [Schimel *et al.*, 1985; Bouwman, 1989; Harden *et al.*, 1999]. Soil decomposition processes must be changed as well owing to the increase (under erosion) or decrease (under deposition) of exposure of SOC in deep layers. The biomass, growth, and death of plant roots must also change dynamically.

[20] In EDCM, up to 10 soil layers can be used to characterize the soil profile. The thickness of the top layer is fixed at 20 cm following the convention of the CENTURY model. This treatment enables EDCM to use the parameter files developed from many applications for CENTURY. The thickness of other soil layers may vary. The initial thickness of each layer is specified in an input file that also specifies information such as bulk density, sand and clay fractions of the soil (texture), and pool sizes of active, slow, and passive SOC in each layer.

4.3. Soil and Carbon Erosion

[21] The rate of soil erosion can be specified monthly using the event schedule file. The thickness of eroded soil is calculated by dividing the eroded soil mass by the bulk density of the topsoil layer. The SOC eroded from the top layer is calculated as

$$C_{erod} = C_{20} * f_{erod} * enrich, \quad (6)$$

where f_{erod} is the fraction of the topsoil layer being eroded, C_{20} is the total amount of SOC in the top 20-cm layer (gC m^{-2}), and “enrich” is an enrichment factor for the SOC in the eroded soil. The enrichment factor, expressed as the ratio of SOC concentration in the eroded soil to that in the topsoil layer, accounts for the fact that soil surface subject to erosion may be enriched in SOC relative to the average of the top 20-cm layer.

[22] To keep the thickness of the top layer constant during erosion, the EDCM model transfers a certain amount of soil to the top layer from the second layer to account for the reduction of thickness caused by erosion. The procedures used in EDCM are similar to the scheme proposed in a number of studies [Schimel *et al.*, 1985; Bouwman, 1989; Harden *et al.*, 1999] and are described in Appendix A. Soil properties in the top layer, such as bulk density and root biomass, are adjusted accordingly using a thickness-weighted approach (see Appendix A).

4.4. Soil and Carbon Deposition

[23] Both the rate of soil deposition and the content of SOC in the deposited materials are specified in order to simulate the SOC dynamics at the depositional sites. The soil deposition rate is used to simulate a change of soil depth. Because of the difficulty in relating eroded sediment to source material and transport on the landscape, we did not attempt to predict the texture of the deposited material. Instead, it is assumed in EDCM that the texture of the deposited soil is the same as the surface soil at the deposition site.

[24] In EDCM, the increase in soil thickness after deposition (d_d or the equivalent thickness of the deposited soil) is estimated as the deposited soil mass per unit area divided by the soil bulk density of the top layer at the deposition site. Before the deposited SOC is added to the top layer, a certain fraction ($= d_d/20$, where 20 is the thickness of the top layer in centimeters) of SOC is subtracted from the top layer and added to the second layer. Accordingly, the thickness of the second layer is increased by the equivalent thickness. The second layer is divided into two layers if it becomes thicker than 20 cm after the addition, with the new third layer

having a thickness of 20 cm. The original third layer becomes the fourth, the fourth becomes the fifth, and so forth. The tenth layer is combined with the ninth layer if necessary. This treatment is to prevent the second layer from becoming too thick, and thus provides a more detailed representation of soil profile near the surface where biological activities are faster than in the deeper layers. The dynamics of SOC, bulk density, soil texture, and plant roots during deposition are adjusted using similar approaches to those described for soil and carbon erosion.

4.5. Comparison Between EDCM and CENTURY V

[25] When this paper was written, a new version of CENTURY (CENTURY V) had been developed (<http://www.nrel.colostate.edu/projects/century5/>). Similar to EDCM, CENTURY V uses a multiple soil-layer model structure to accommodate vertical variability of soil texture, bulk density, wilting point, field capacity, and percent soil organic matter. CENTURY V can simulate the impacts of both erosion and deposition. Nevertheless, there are fundamental differences between EDCM and CENTURY V.

[26] EDCM simulates SOC dynamics in each layer independently with layer-dependent biogeochemical processes and properties, while CENTURY V calculates the SOC profile as a function of the SOC content in the top layer and soil depth. The biogeochemical processes including carbon dynamics are simulated only in the top layer. Apparently, the CENTURY V approach is not intrinsically dynamic because it assumes that the SOC distribution in soil profiles follows an exponential decay function that is static over time and thus does not allow for SOC distribution patterns to change over time. In EDCM, SOC vertical distribution patterns can be altered by changes in rooting properties and soil erosion and deposition. The CENTURY V exponential decay pattern of SOC with depth might not hold under deposition environments in which SOC content in the top layer might be lower than those in deep layers.

[27] Compared with the dynamic representation of the evolution of soil profiles in EDCM, CENTURY V uses three layers to simulate carbon dynamics under erosion and deposition. The top simulation layer varies from 20 to 50 cm. Since the lower layer depth is fixed at 200 cm, pools of infinite capacity (i.e., the third layer) are used to provide or accept material in the lower layer as the lower layer thickness expands or contracts. Although CENTURY V is able to track the evolution of soil depth under erosion or deposition, it has limited capability in simulating SOC dynamics in the entire profile because SOC changes in the deep layers are calculated without consideration of various dynamic processes in these layers.

5. Model Parameterization

[28] Most of the input files for EDCM were taken directly from Sharpe *et al.* [1998] and Harden *et al.* [1999]. Modifications are described below.

5.1. Soil Profile Initialization and Spin-Up Run

[29] To accommodate the observed SOC profiles and the rooting depth of temperate trees [Jackson *et al.*, 1996], 10 layers (20 cm each) with a total depth of 2 m were used for

all model simulations. Probably owing to the presence of a fragipan, field measurements of SOC were only taken to a depth of 60 cm at the ridge top in the hardwood forest at Goodwin Creek. The existence of a fragipan, however, might not be a physical limitation for root penetration because considerable amounts of SOC were observed below the fragipan [Harden *et al.*, 1999].

[30] Initial conditions specified for each of the soil layers include thickness, contents of five SOC pools, bulk density, and fractions of sand, silt, and clay in each layer. The vertical distribution of tree roots was predicted using the general equation for temperate trees [Jackson *et al.*, 1996]. The SOC values in each of the five SOC pools were generated from a 10,000-year spin-up run in which the modeled system reaches an equilibrium condition. Several spin-up runs were performed, with adjustment of the depth-dependent soil aeration parameters to give the best agreement with the observed ridge top SOC profile.

5.2. Characteristics of Crops

5.2.1. Vertical Distribution of Roots

[31] Land cover change is usually accompanied by changes in rooting pattern, which in turn affects the allocation of net primary productivity (NPP) into the soil profile. The vertical distribution of roots for crops was predicted based on a normalized function derived from Buyanovsky and Wagner [1986]. The normalized grass root distribution was from Jackson *et al.* [1996].

5.2.2. Historical Change of Harvest Index

[32] In EDCM, NPP and plant residue return are related to historical changes of harvest index and grain yield (see Appendix A). Harvest index is defined as the ratio of grain biomass to aboveground biomass. The maximum harvest index, inherited from CENTURY, is a static input parameter in EDCM. We assumed that the maximum harvest index for each crop species in the default CENTURY crop input file represents the value around 1995. The maximum harvest index (H_i) at each point in time was derived from this 1995 value using empirical formulas described below. The realized harvest index, which is simulated in EDCM, depends on the maximum H_i , nutrients, and water availability during the growing season.

[33] Extensive increases of maximum or potential harvest index due to genetic improvements over time have been reported for various crops [Austin *et al.*, 1980; Wych and Rasmusson, 1983; Cox *et al.*, 1988; Russel, 1991; Rooney and Leigh, 1993; Hay, 1995; Voldeng *et al.*, 1997; Sinclair, 1998]. The harvest index of winter wheat from 1900 to 1988 increased at a rate of 0.0016 yr^{-1} ($r^2 = 0.68$) according to the data of Cox *et al.* [1988]. In this study, we assumed that the historical changes of potential H_i for all crops follow the pattern of winter wheat cultivars as observed by Cox *et al.* [1988]. This assumption was supported by the increase rate of 0.0017 yr^{-1} observed in corn from 1960 to 1992 [Huggins and Fuchs, 1997], $0.0012\text{--}0.0024 \text{ yr}^{-1}$ for wheat [Austin *et al.*, 1980; Riggs *et al.*, 1981; Wych and Rasmusson, 1983], and others summarized by Hay [1995]. We assumed that the potential harvest index for a specific crop was constant before 1900, which was consistent with observations [Rooney and Leigh, 1993].

5.2.3. Historical Change of Grain Yield

[34] We have shown that the historical patterns of harvest index and grain yield are both important constraints in estimating the amount of plant residue returned to the soil (see Appendix A). From 1870 to 1997, crop yields increased dramatically in the United States because of changes in crop genetics, harvest index, fertilization, and cropping practices. To incorporate these trends into the EDCM, we fitted a time-dependent logistic growth function for each crop using the historical, statewide, annual mean yield data of the crop compiled by the U.S. Department of Agriculture National Agricultural Statistics Service (<http://www.usda.gov/nass/>). These derived functions, along with the temporal change of harvest index, were then used for estimating the historical change of potential primary productivity for various crops.

5.3. Soil Erosion and Deposition

[35] The erosion rates during various periods were documented by Harden *et al.* [1999] and are listed in Table 1. Erosion rates were compiled from different sources, including measurements collected at the Nelson Farm and other references nearby. Because of the uncertainty in erosion history, two sets of rates representing the maximum and minimum scenarios were provided. Soil and crop management practices, along with precipitation variability, were used to guide the estimation of the range and changes of soil erosion rates over time.

[36] Using the SOC content in the top 2.5 cm of soil, Starr *et al.* [2000] derived an enrichment factor (“enrich”) of 2.1 in two conservation tillage watersheds in Ohio, on the basis of 12 years of observations. Collins *et al.* [1997] showed that relating eroded sediment to source material in intermediate-sized watersheds (10-km scale) was complex and difficult. They reported that the enrichment factor ranged from 0.5 to greater than 5, depending on whether the eroding site was stream bank, forest, pasture, or cultivated soil. A value of 2 was used for the enrichment factor in this study.

[37] Because deposition rates were not measured at Nelson Farm, we set maximum and minimum scenarios for soil deposition to correspond to the mass soil and SOC erosion rates of the maximum and minimum erosion scenarios. This approach would be equivalent to assuming equal areas of erosion and deposition, and no loss of SOC during transport, if we were to balance soil and SOC mass between erosional and depositional sites. Although these assumptions are not likely at the landscape scale, they provide a basis for comparison of the effects of specific erosional soil loss with the equivalent depositional soil accretion.

5.4. Management Practices

[38] Management practices, such as crop transition, cultivation, fertilization, and harvesting method, were taken from Harden *et al.* [1999] and Sharpe *et al.* [1998] and are listed in Table 1.

6. Model Calibration, Validation, and Sensitivity Analysis

[39] Historical grain yields and the vertical distribution of SOC as measured at the ridge top were used to calibrate two

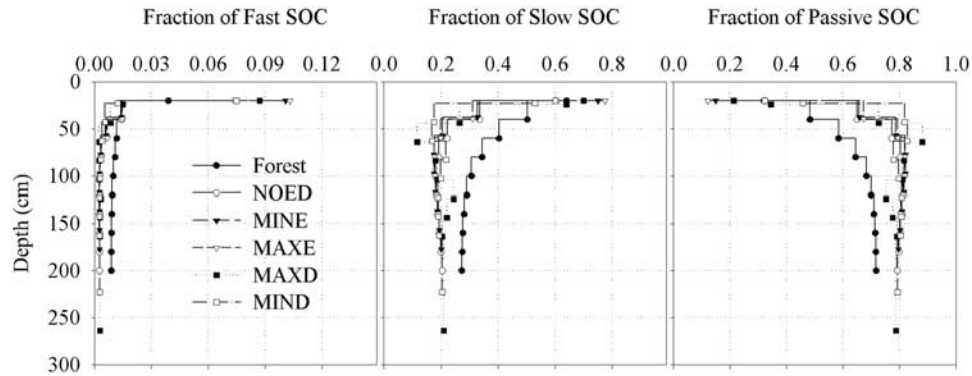


Figure 1. Simulated vertical distributions of fractions of active, slow, and passive soil organic carbon in soil profile for the forest (in 1870) and croplands under various erosion and deposition scenarios. No erosion or deposition was specified under forest and NOED during model simulation. MINE and MAXE represented minimum and maximum erosion scenarios, while MIND and MAXD corresponded to minimum and maximum deposition scenarios, respectively.

sets of model parameters. First, the normalized general trends of historical yield of different crops were derived from national data sets, and they might be different from those at Nelson Farm. The parameters of the logistic growth function were adjusted, if necessary, to catch the general trends of measured crop yield at Nelson Farm. It is vitally important that the model can realistically catch the temporal change of grain yield and therefore correctly estimate the dynamic change of plant residue input into the soil system over time. Second, the parameters in the equation that describes the decrease of soil aeration with depth (see Appendix A) were calibrated using the observed vertical distribution of SOC at the ridge.

[40] The model was validated using field measurements of soil moisture, soil temperature, and the vertical distribution of SOC as measured in 1996 at the eroding and depositional sites. The following model runs were performed to carry our analysis from spin-up through calibration to scenario development.

[41] 1. In the spin-up forest run we used the parameter set developed for the Coweeta broadleaved forests by the CENTURY staff. Model calibration was performed on the vertical distribution of SOC. The purpose of the spin-up run is to generate an initial allocation of SOC to the five pools (metabolic, structural, active, slow, and passive) for each soil layer for subsequent runs that introduce human disturbances (from 1870 to 1997).

[42] 2. In the scenario with no erosion or deposition (NOED), starting from the results generated from the spin-up run (representing the forest around 1870), EDCM was run for the Nelson Farm ridge top with all the historical management and cropping practices but without soil erosion or deposition. Model calibration on grain yield was performed in this run.

[43] 3. In the minimum erosion scenario (MINE), all the conditions and inputs were the same as for NOED except that the minimum erosion scenario was used (Table 1, minimum erosion column).

[44] 4. In the minimum deposition scenario (MIND), all the conditions and inputs were the same as for NOED except that the minimum deposition scenario was used.

[45] 5. In the maximum erosion scenario (MAXE), all the conditions and inputs were the same as for NOED except that the maximum erosion scenario was used (Table 1, maximum erosion column).

[46] 6. In the maximum deposition scenario (MAXD), all the conditions and inputs were the same as for NOED except that the maximum deposition scenario was used.

[47] The baselines for the sensitivity analysis were MINE for erosion simulations and MIND for deposition simulations. In the sensitivity analysis, the following input parameters and drivers were altered by -10% or $+10\%$ one at a time: initial SOC quantity and quality, soil texture, precipitation, temperature, potential primary productivity, vertical allocation of NPP to roots, and erosion and deposition rates. The sensitivity of the following variables to the prescribed changes was analyzed: NPP, grain production, the vertical change of SOC, cumulative CO_2 emissions during the entire simulation period, and the importance of deep soil layers in accounting for SOC change in soil.

7. Results

7.1. Spin-Up Forest Run

[48] The simulated NPP for the forest under equilibrium conditions was $350 \text{ gC m}^{-2} \text{ yr}^{-1}$, which was in good agreement with the field measurement of $335 \text{ gC m}^{-2} \text{ yr}^{-1}$. The simulated total SOC in the top 20-cm layer was 3180 gC m^{-2} , which compares well with the field measurement of 3278 gC m^{-2} at the ridge top. The simulated SOC in the second and third layers was 727 gC m^{-2} and 679 gC m^{-2} , which compares well with field measurements of 872 gC m^{-2} and 793 gC m^{-2} , respectively. Figure 1 shows the simulated vertical distributions of fast, slow, and passive SOC in the profile, which are consistent with field observations [Harrison *et al.*, 1993; Van Dam *et al.*, 1997].

7.2. Evolution of Soil Depth and SOC Erosion

[49] The initial soil depth was set at 200.0 cm and remained constant for the NOED case. Soil depth at the end of the simulation was 177 cm and 139 cm, respectively, under MINE and MAXE, representing a change of 23 cm

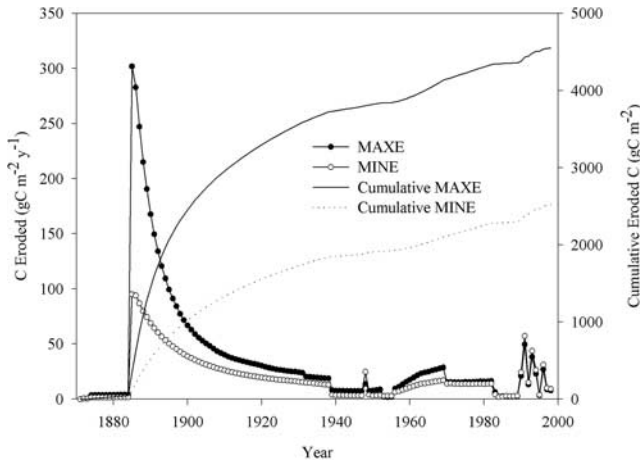


Figure 2. Annual and cumulative soil organic carbon (SOC) erosion from 1870 to 1997 under minimum (MINE) and maximum (MAXE) erosion scenarios.

and 61 cm, respectively, during the 128 years. The original top 20-cm layer was completely eroded under both scenarios. The depth in 1997 was 223 cm and 264 cm under MIND and MAXD, respectively. The minor difference between the gain (deposition) and loss (erosion) in soil depth was caused by the difference of bulk density in the profiles.

[50] Overall, about 2452 and 4403 gC m^{-2} were eroded between 1870 and 1997 under MINE and MAXE, respectively (Figure 2). The SOC erosion rate immediately after the pasture-cropland conversion greatly increased to about $100 \text{ gC m}^{-2} \text{ yr}^{-1}$ under MINE or $300 \text{ gC m}^{-2} \text{ yr}^{-1}$ under MAXE, and then decreased gradually afterward, mainly owing to the reduction of SOC percentage in the top layer caused by previous erosion (SOC decreases with depth) and crop harvesting. The massive SOC erosion between 1872

and 1910 accounted for about half of the total SOC eroded during the entire simulation period (128 years). Because the amount of SOC eroded was calculated as the product of the amount of soil eroded and the corresponding content of SOC in the top layer, and because the SOC content under MINE was consistently higher than that under MAXE, more SOC could be eroded under MINE during certain time periods when soil erosion rates were close under both scenarios (Figure 2).

7.3. Soil Moisture, Soil Temperature, and Grain Yield

[51] The seasonal dynamics of soil moisture content and temperature in the first layer were well simulated by EDCM (Figure 3). It was difficult to do a statistical assessment on model performance because field measurements were sporadic in time, while model simulations were at monthly time steps. EDCM captured the general historical pattern of crop yield as observed in average yields for different periods at Nelson Farm from 1884 to 1997 (Figure 4, RMSE = 1.2 to $7.4 \text{ gC m}^{-2} \text{ yr}^{-1}$). Annual variability of soybean yield from 1990 to 1997 under the minimum erosion scenario was also well simulated (Figure 4, RMSE = 15.2 to $16.1 \text{ gC m}^{-2} \text{ yr}^{-1}$). Simulated grain yield decreased 18% and 3%, respectively, under MAXE and MINE compared with that under NOED during the entire simulation period. Soil deposition had no apparent impact on grain yield. The simulated effects were consistent with field studies [Frye et al., 1982; Schertz, 1989; Mokma and Sietz, 1992; Malhi et al., 1994; Schumacher et al., 1994]. Schertz [1989] reported that corn yields under a severe erosion phase decreased 15% and 10% compared with the slight and moderate erosion phases, respectively, over a 6-year period (1981–1986) for three Indiana soils. Mokma and Sietz [1992] reported that 5-year corn averages for severely eroded plots on Marlette soil in Michigan were 21% less than those for slightly eroded plots. Reduced yield on eroded soils can be explained by a variety of factors,

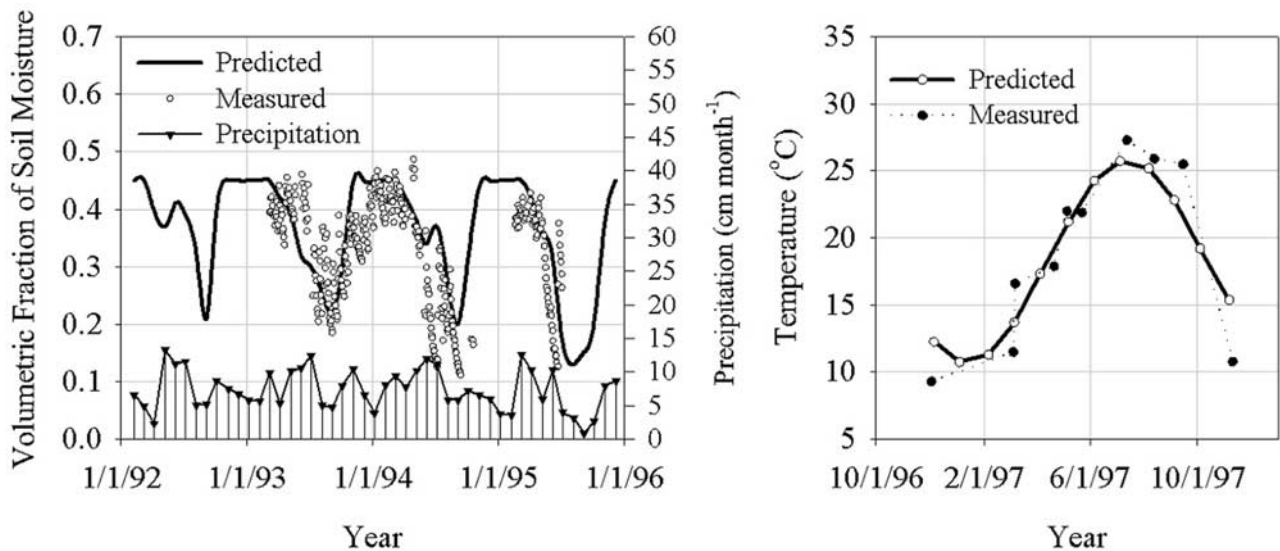


Figure 3. Comparison of simulated and measured volumetric soil moisture content and soil temperature in the surface layer at Nelson Farm.

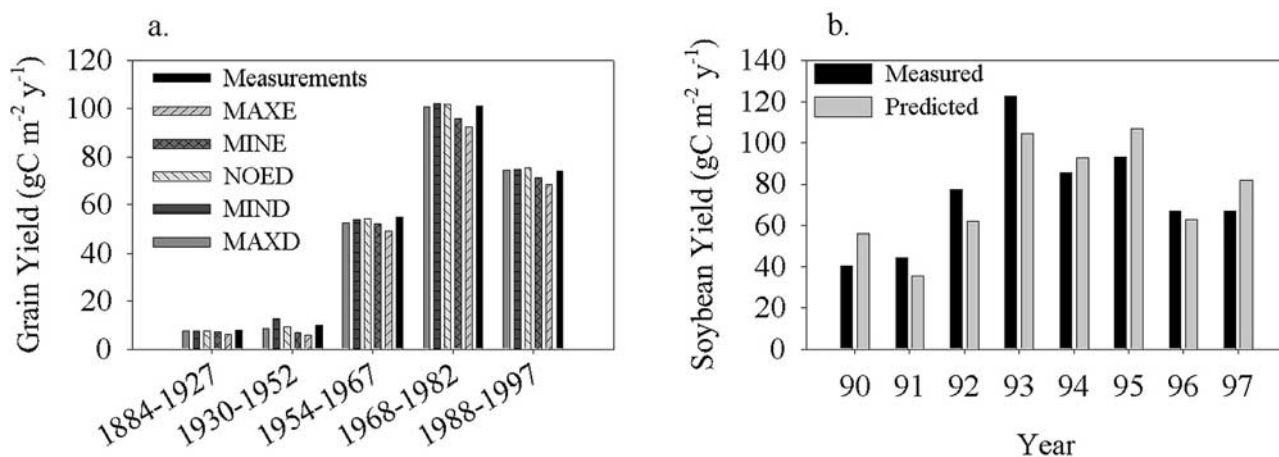


Figure 4. Comparison of simulated and measured grain yield at Nelson Farm under various erosion and deposition scenarios. (a) Average yields during different periods from 1884 to 1997. (b) Annual variation of soybean yield from 1990 to 1997.

including lower organic matter content, higher soil bulk density, and lower amounts of soil nutrients [Frye *et al.*, 1982; Schertz, 1989].

7.4. SOC Dynamics in the Top 20-cm Layer

[52] After pasture was converted to cropland in 1883, SOC dynamics could be characterized by two distinct periods: depletion (1883–1950) and recovery (1950–1997). SOC depletion from 1883 to 1950 was caused by grain and straw harvest and severe soil erosion. At the end of this period, top-layer SOC had been reduced significantly, ranging from 2021 gC m⁻² (63% loss) under MIND to 2913 gC m⁻² (91% loss) under MAXE (Figure 5). The SOC contents in the top layer around 1950 were in the following descending order: MIND, NOED, MAXD, MINE, and MAXE. SOC under MAXD was initially higher than in all other scenarios because of massive deposition of SOC, but then it gradually became lower than those under MIND and NOED because the deposited materials (derived from the MAXE scenario) had less SOC than those on the MIND and NOED scenarios (Figure 5). Both slow and passive SOC demonstrated depletion patterns similar to the total SOC (Figure 5). However, the depletion of slow SOC was more dramatic than the passive SOC. About 89% to 96% of the initial slow top-layer SOC was depleted at the end of this period, whereas the reduction of passive SOC ranged from 7% (MIND) to 81% (MAXE). The reduction of passive SOC under MAXD was not caused by decomposition as much as by dilution by deposition of materials with less passive SOC content. The fast depletion of passive SOC in the eroding scenarios was caused by soil erosion.

[53] The SOC recovery period started in 1950 when carbon flux into the top layer became positive owing to intensification of fertilization, use of genetically improved crops, and improved cropping practices, such as the retention of plant residue after harvest (Table 1). During this period, the largest SOC increase was found under MAXD, followed by MIND, NOED, MAXE, and MINE. The majority of the SOC increase in the top layer was caused

by the increase of slow SOC (Figure 5, panel A2). Passive SOC was relatively stable during this period (Figure 5, panel A3). The simulated top-layer SOC in 1997 under NOED was 2709 gC m⁻², compared with 2499 gC m⁻² as observed at the Nelson Farm ridge-top site.

[54] The simulated top-layer SOC under erosion scenarios ranged from 1816 to 1919 gC m⁻², higher than field measurements of 1142 to 1518 gC m⁻² taken at three upper slope positions [Harden *et al.*, 1999]. The significant difference between the simulated and measured SOC in the top layer might be caused by a number of factors. The actual erosion rates might have been higher than the rates specified, or a fraction of the nutrients added to these sites by fertilization might have been eroded and thus unavailable to the nutrient pools in this study, contributing to the overestimation of primary production and SOC stock on these sites. The simulated SOC under deposition scenarios ranged from 2458 to 2902 gC m⁻², within the range of field measurements of 2410 ± 438 (standard deviation) gC m⁻² from three lower slope positions.

[55] SOC quality in the top layer experienced dramatic temporal changes (Figure 6). Before 1950, the fraction of slow top-layer SOC decreased from 63% to less than 20%, while the fraction of passive SOC increased proportionally. The fraction of active SOC remained relatively stable at around 3%. Since 1950, the fraction of active top-layer SOC increased up to 20% under MAXE, and the fraction of slow SOC increased steadily, indicating a steady increase of plant residue input into the soil. Consequently, the fraction of passive SOC decreased proportionally. Fractions of passive top-layer SOC ranged from 16% (MAXE) to 45% (NOED). Results indicated that top-layer SOC in the erosional scenarios was more labile than that in the NOED and MIND scenarios.

7.5. SOC Dynamics in Soil Profiles

[56] Similarly to the temporal patterns of SOC in the top layer, two distinct periods could be found in the temporal changes of SOC in the whole soil profile (Figure 5). In the

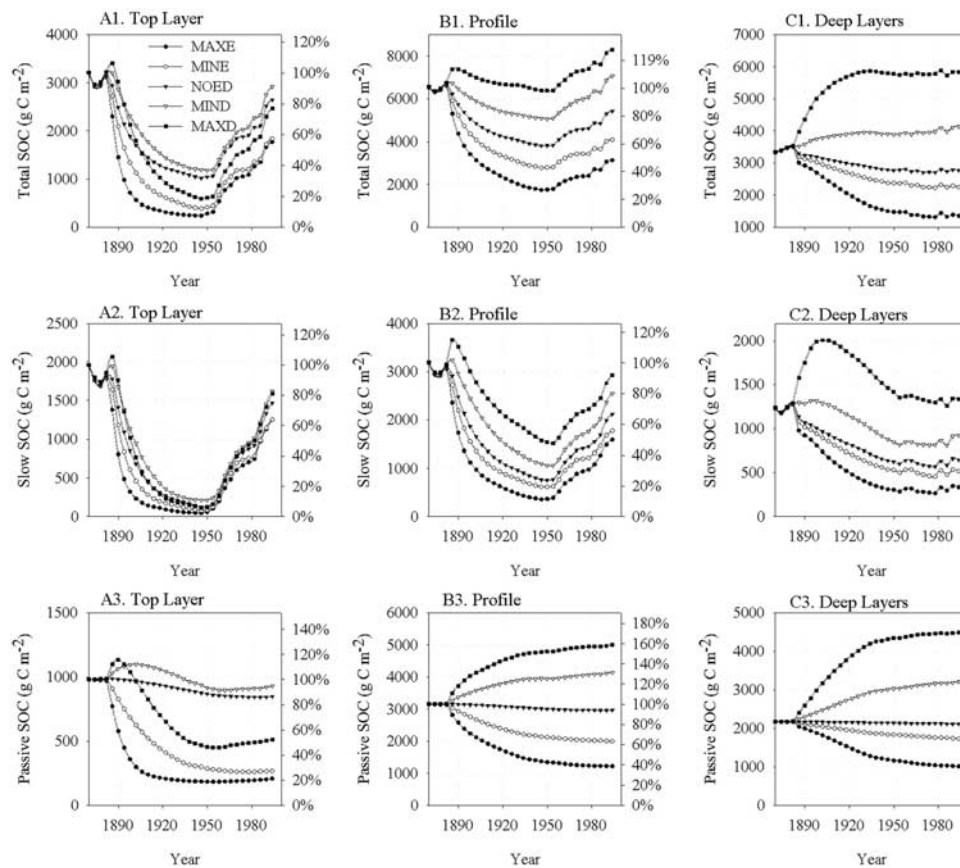


Figure 5. Simulated historical trajectories of total soil organic carbon (SOC), slow, and passive SOC pools in the top 0.2-m soil layer (A1–A3), the whole profile (B1–B3), and the deep layers (20 to 200 cm) under various erosion and deposition scenarios. Two periods could be identified to characterize the SOC change in the top and entire profile: depletion (from start of cultivation to 1950) and recovery (from 1950 to 1997).

depletion period (1883–1950), SOC was reduced in all scenarios (Table 2). The SOC loss ranged from 194 gC m^{-2} (MAXD) to 4807 gC m^{-2} (MAXE). Most of the SOC loss was accounted for by the reduction of slow C, ranging from 1642 to 2844 gC m^{-2} (Figure 5). The passive C decreased under MAXE, MINE, and NOED, while it increased under deposition scenarios. In the recovery period (1950–1997), SOC gain happened in all scenarios, varying from 1396 gC m^{-2} ($30 \text{ gC m}^{-2} \text{ yr}^{-1}$) for MINE to 1942 gC m^{-2} ($41 \text{ gC m}^{-2} \text{ yr}^{-1}$) for MIND (Table 3). SOC contents varied from 3178 gC m^{-2} for MAXE to 8222 gC m^{-2} for MAXD in 1997 (Table 2), suggesting SOC gains in the depositional scenarios and SOC loss in the control and erosional scenarios.

[57] Deposition increased the amount of slow C most dramatically in the deep layers under MAXD. This response was caused by the dramatically increased deposition (Figure 2) that effectively accelerates the burial of SOC in the deep layers because the thickness of the surface layer was set constant. Any deposition causes vertical transport of SOC in the model, and SOC is less susceptible to decomposition as it becomes buried in deeper layers.

[58] Metrics of the impact of erosion on SOC were negative in both eroding scenarios for both periods (i.e., 1870 to 1950 and 1950 to 1997) (Table 2). The ψ values

under MAXE and MINE from 1870 to 1950 were -2059 gC m^{-2} ($-26 \text{ gC m}^{-2} \text{ yr}^{-1}$) and -1030 gC m^{-2} ($-13 \text{ gC m}^{-2} \text{ yr}^{-1}$), respectively, representing 31% and 16% more SOC loss than in the NOED scenario. The ψ values under MIND and MAXD were positive, indicating a comparative SOC increase in the depositional scenarios. The impacts of erosion on SOC ranged from -10 to $-18 \text{ gC m}^{-2} \text{ yr}^{-1}$, while that of deposition varied from 12 to $23 \text{ gC m}^{-2} \text{ yr}^{-1}$ during the entire simulation period. The simulated negative impact of soil erosion and positive impact of deposition on SOC in the profile were consistent with field measurements [Slater and Carleton, 1938; Harden et al., 1999].

[59] The quality of SOC in the deep layers changes significantly in all scenarios (Figure 6), although not as dramatically as in the top layer. In 1870, the slow C accounted for approximately 50% of the total SOC, but by 1950 it accounted for only about 20% under all scenarios, and then increased to values between 26% and 44%. The temporal change of the fraction of the passive SOC was the opposite of slow SOC. The fast SOC accounted for less than 10% for most of the time. At the end of the simulation, the quality of the SOC profile had changed significantly compared with the initial quality (Figure 1). This change probably reflects the change induced by different rooting

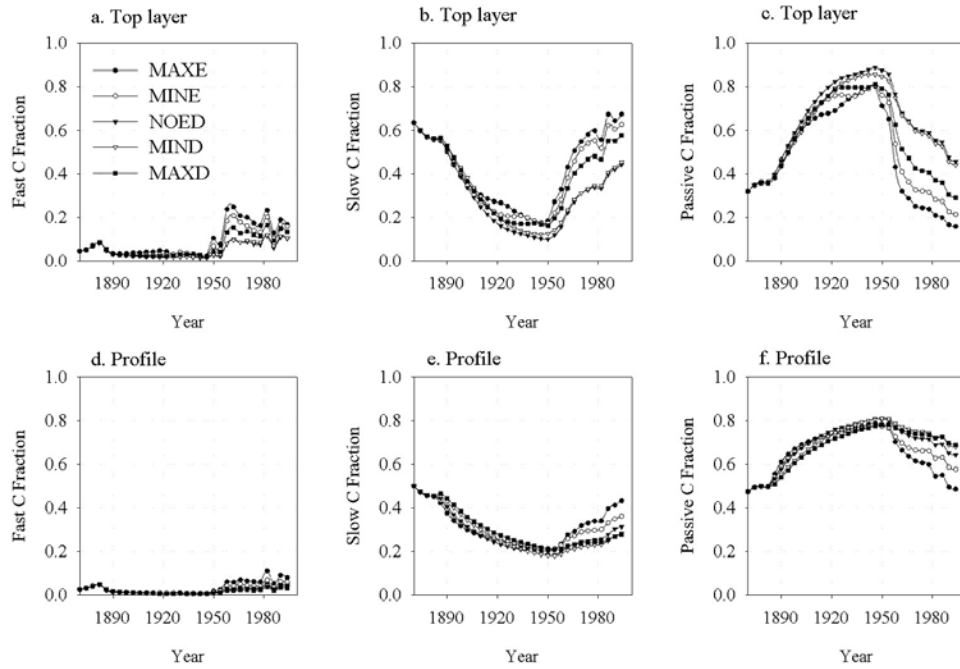


Figure 6. Simulated temporal change of the soil organic carbon (SOC) quality (i.e., the composition of the fast, slow, and passive soil organic carbon pools) in (top) the top 20-cm layer and (bottom) the whole profile from 1870 to 1997.

properties of trees and crops, as well as the impact of soil erosion and deposition. Tree roots penetrate more deeply into the profile, and therefore the fractions of the slow and active pools in the deep layers would be larger under forests than under crops.

7.6. C Source or Sink

[60] The strengths of C source or sink (Φ) were calculated on the basis of mass conservation according to equation (2). All sites acted as C sources to the atmosphere CO_2 from 1870 to 1950 with source strengths ranging from 13 to 49 $\text{gC m}^{-2} \text{yr}^{-1}$ (Table 4). The C source strengths had this ascending order: MAXE, MINE, NOED, MIND, and MAXD. All sites became C sinks (26 to 44 $\text{gC m}^{-2} \text{yr}^{-1}$) from 1950 to 1997 with the highest sink strength found

under MAXE and lowest under MAXD (Table 3). During the entire simulation period (1870 to 1997), the eroding scenarios acted as C sinks with sink strengths ranging from 1 to 8 $\text{gC m}^{-2} \text{yr}^{-1}$, while the control and depositional scenarios were C sources (Table 4).

[61] The Ω values measuring the impact of erosion or deposition on C source or sink are shown in Table 4. The Ω values were positive in the eroding scenarios during both time periods (i.e., 1870 to 1950 and 1870 to 1997), indicating erosion reduced their C source strengths from 1870 to 1950 and enhanced their C sink strengths from 1950 to 1997. This interpretation is based on previous findings that all scenarios were C sources from 1870 to 1950 and they were C sinks from 1950 to 1997. In contrast, the Ω values for the depositional scenarios were all negative

Table 2. Loss or Gain of Soil Organic Carbon (SOC) and the Impact of Soil Erosion and Deposition on SOC Storage (ψ_i) in the Whole Profile Under Various Erosion and Deposition Scenarios Compared With the Presettlement Conditions

Scenario	Year	SOC, gC m^{-2}	SOC Change			Impact of Erosion or Deposition on SOC: ψ_i		
			Total, ^a gC m^{-2}	Annualized Rate, $\text{GGG m}^{-2} \text{yr}^{-1}$	% of Initial	Total, gC m^{-2}	Rate, $\text{gC m}^{-2} \text{yr}^{-1}$	% of Initial
Initial	1870	6558						
MAXE	1950	1751	-4807	-60.1	-73.3	-2059	-25.7	-31.4
MINE	1950	2780	-3778	-47.2	-57.6	-1030	-12.9	-15.7
NOED	1950	3810	-2748	-34.4	-41.9	0	0.0	0.0
MIND	1950	5081	-1477	-18.5	-22.5	1271	15.9	19.4
MAXD	1950	6364	-194	-2.4	-3.0	2554	31.9	38.9
MAXE	1997	3178	-3380	-42.3	-51.5	-2292	-18.0	-34.9
MINE	1997	4176	-2382	-29.8	-36.3	-1294	-10.2	-19.7
NOED	1997	5470	-1088	-13.6	-16.6	0	0.0	0.0
MIND	1997	7023	465	5.8	7.1	1553	12.2	23.7
MAXD	1997	8222	1664	20.8	25.4	2752	21.7	42.0

^aEquivalent to the integration of dC/dt over the period of simulation.

Table 3. Contemporary (1950–1997) Change of Soil Organic Carbon in the Whole Profile and Strength of Carbon Sequestration in Cropland Soils Under the Impact of Soil Erosion and Deposition

Scenario	SOC Change From 1950 to 1997		Eroded (–) or deposited (+) SOC, gC m ⁻²	C Sink Φ	
	Total, gC m ⁻²	Rate, gC m ⁻² yr ⁻¹		Total, gC m ⁻²	Rate gC m ⁻² yr ⁻¹
MAXE	1427	30.4	–651	2078	44.2
MINE	1396	29.7	–565	1961	41.7
NOED	1660	35.3	0	1660	35.3
MIND	1942	41.3	565	1377	29.3
MAXD	1858	39.5	651	1207	25.7

for both periods, showing enhanced release of C from the soil to the atmosphere in these scenarios. In the MAXD case, the carbon content of the soil increased from 6558 gC m⁻² in 1870 to 8222 gC m⁻² in 1997. The magnitude of increase was smaller than the total depositional C input of 4403 gC m⁻², suggesting that not all SOC deposited could be protected from decomposition and the scenario acted as a C source of 2739 gC m⁻². The depositional scenarios have more carbon available for decomposition and, therefore, larger emission rates.

7.7. Sensitivity Analysis

[62] The results of a sensitivity analysis of the EDCM model under the MINE scenario are listed in Table 5. Descriptions of Table 5 are given in Appendix A. The sensitivity of EDCM under the minimum depositional case MIND was roughly similar to its sensitivity under the minimum erosional case MINE, with some difference in magnitude (see Appendix A).

8. Discussion

8.1. SOC Dynamics Under Erosion or Deposition

[63] The predicted general pattern of SOC dynamics following the conversion of forests to croplands was in agreement with both field observations [Buyanovsky and Wagner, 1998b] and previous modeling results [Donigian et al., 1994; Harden et al., 1999], although the exact trajectories may differ. Few studies have been designed for the purpose of observing SOC change driven by erosion and

deposition. Owing to the difficulty of long-term monitoring at the watershed scale, field studies that were designed to assess the impact of soil erosion and deposition used a paired-plot approach or a toposequence approach [Slater and Carleton, 1938; Webber, 1964; Schimel et al., 1985; Harden et al., 1999]. Field measurements were taken from several topographic positions that experienced various degrees of soil erosion or deposition, and the difference in SOC storage was attributed to either soil erosion or deposition. As indicated by our simulated results (Figure 5), a couple of points selected from the SOC trajectories would not reveal many important processes. Capturing the dynamics of SOC under the influence of erosion or deposition requires that soil and SOC erosion or deposition, as well as SOC content, be monitored during long-term studies.

8.2. Importance of the Whole-Profile Approach

[64] It is essentially impossible to evaluate the overall impact of soil erosion and deposition if we only observe the change in SOC in the top layer or couple of layers, without observing the SOC change in the whole profile. Erosion and deposition can change the depth as well as the soil properties and processes within the profile. The whole-profile approach simulates the dynamics of the entire profile and therefore provides a suitable framework for assessing the impact of soil erosion and deposition. The metrics measuring the impacts of soil erosion and deposition should not be applied to a single layer that has experienced dynamic replacement of soil.

[65] It has been shown by this study and in field observations [Harrison et al., 1993; Van Dam et al., 1997] that SOC quality changes with depth (Figure 1). The fraction of labile SOC (i.e., active pools) decreases with increasing soil depth. This distribution pattern could be altered by land cover change (especially with changes in rooting properties), as well as by soil erosion and deposition. Without incorporating the changes in SOC quality, we would introduce biases into the SOC decomposition and therefore the simulation of the entire ecosystem. Omitting explicit consideration of the change of the fractions of various SOC pools in the soil profile might lead to overestimating SOC oxidation [Voroney et al., 1981] and nitrogen mineralization [Hadas et al., 1989] in deep layers.

Table 4. Exchange Rates of C Between the Soil and Atmosphere (Φ), and the Impacts of Soil Erosion and Deposition on Sources/Sinks (Ω) During Two Time Periods (1870 to 1950 and 1870 to 1997)

Scenario	Year	SOC, gC m ⁻²	Total SOC Eroded (–) or Deposited (+) C _v , gC m ⁻²	Sink (+) or Source (–) Φ		Impact of Erosion or Deposition on Source/Sink: Ω		
				Total, gC m ⁻²	Rate, gC m ⁻² yr ⁻¹	Total, gC m ⁻²	Rate, gC m ⁻² yr ⁻¹	% of Initial
Initial	1870	6558						
MAXE	1950	1751	–3752	–1055	–13.2	1693	21.2	25.8
MINE	1950	2780	–1887	–1891	–23.6	857	10.7	13.1
NOED	1950	3810	0	–2748	–34.4	0	0.0	0.0
MIND	1950	5081	1887	–3364	–42.1	–616	–7.7	–9.4
MAXD	1950	6364	3752	–3946	–49.3	–1198	–15.0	–18.3
MAXE	1997	3178	–4403	1023	8.1	2111	16.6	32.2
MINE	1997	4176	–2452	70	0.6	1158	9.1	17.7
NOED	1997	5470	0	–1088	–8.6	0	0.0	0.0
MIND	1997	7023	2452	–1987	–15.6	–899	–7.1	–13.7
MAXD	1997	8222	4403	–2739	–21.6	–1651	–13.0	–25.2

Table 5. Sensitivity of Some of the Output Variables to Input Variables as Represented by the EDCM Model Under the Minimum Erosion Scenario^a

Variable	Change, %	NPP ^b	Grain, gC m ⁻²	Straw, gC m ⁻²	C Eroded, gC m ⁻²	Depth, cm	SOC in Profile, gC m ⁻²			SOC in Top 20 cm, gC m ⁻²			Cumulative Gross CO ₂ Emission, gC m ⁻²	
							Total	Slow	Passive	Total	Slow	Passive	0–20 cm	Deep Layers
Baseline (MINE)		178	3296	1583	2452	177.2	4176	1846	1996	1959	1366	273	14180	2256
Initial SOC	10	0.0	0.2	0.8	6.2	0.0	5.4	1.6	9.7	1.2	0.1	7.7	1.7	4.8
	-10	-0.6	-0.2	-0.8	-6.2	0.0	-5.4	-1.7	-9.7	-1.2	-0.1	-8.1	-1.7	-4.8
Initial SOC quality ^c	(1)	0.0	0.1	0.1	-6.6	0.0	-2.3	1.4	-6.0	-1.6	-0.1	-11.7	1.3	4.8
	(2)	0.6	0.0	-0.2	5.1	0.0	1.7	-1.4	4.9	1.3	0.0	8.8	-1.3	-4.0
Soil Erosion Rate	10	-1.7	-1.4	-1.8	6.0	-1.5	-2.8	-3.0	-2.8	-2.7	-2.6	-4.4	-1.5	-1.6
	-10	-0.6	0.3	0.6	-6.6	1.3	2.6	2.8	2.8	3.3	3.7	4.4	0.1	0.0
PPP	10	9.6	9.4	6.4	5.3	0.0	4.7	8.0	0.3	9.5	10.1	1.8	8.4	6.3
	-10	-10.7	-11.1	-7.3	-4.8	0.0	-6.0	-10.7	-0.4	-11.7	-13.0	-2.6	-8.6	-5.8
β (roots) ^d	(1)	6.2	0.7	1.3	3.7	0.0	1.2	2.1	0.2	0.0	-0.4	0.4	4.0	25.4
	(2)	-9.6	-4.9	-4.2	-4.9	0.0	-3.7	-7.3	-0.3	-5.3	-6.3	-1.5	-6.9	-19.1
Aeration index	10	0.6	0.0	-0.1	-0.2	0.0	-1.1	-1.7	-0.7	-0.2	-0.1	-0.7	-0.1	2.6
	-10	0.0	0.1	0.2	0.4	0.0	1.2	2.0	0.7	0.2	0.1	0.7	0.1	-3.2
Enrichment factor	10	-0.6	-0.3	-1.0	5.4	0.0	-1.1	-1.0	-1.4	-2.3	-1.2	-10.3	-0.9	-0.2
	-10	0.0	0.3	1.0	-5.8	0.0	1.2	1.0	1.6	2.7	1.3	11.7	0.9	0.2
Clay ^e	(1)	-1.1	-1.1	-0.7	-0.3	0.0	0.4	0.5	0.4	-0.6	-1.0	1.1	-0.8	-2.0
	(2)	1.1	1.1	0.8	0.0	0.0	0.0	0.3	-0.5	1.1	1.7	-1.5	1.1	2.4
Bulk density	10	-5.1	-4.6	-2.7	-6.3	1.2	6.4	10.3	3.8	-0.7	-1.3	3.7	-3.9	-15.2
	-10	3.4	3.1	1.7	7.7	-1.4	-5.7	-8.1	-4.5	-0.9	-0.6	-4.8	2.7	9.8
Temperature	5	-8.4	-12.8	-4.8	-2.6	0.0	-7.2	-12.9	-0.6	-13.2	-14.9	-2.9	-6.5	-1.6
	-5	3.9	8.3	2.4	1.7	0.0	4.4	7.2	0.4	8.1	8.3	1.5	3.3	-0.6
Precipitation	5	2.2	3.3	1.9	0.4	0.0	0.3	0.8	0.1	0.5	0.8	0.4	2.2	0.9
	-5	-2.8	-3.1	-1.7	-0.1	0.0	-0.7	-1.3	-0.1	-1.3	-1.5	-0.7	-2.2	-1.1

^aAll values except for the baseline are percentage change relative to the baseline scenario.

^bNPP is the average net primary productivity from 1870 to 1997 in gC m⁻² yr⁻¹; the following variables were expressed as cumulative during the simulation period: grain and straw harvested, C eroded and CO₂ effluxes; soil depth, total, slow, and passive SOC represented the values at the end of the simulation.

^c(1)slow C increased 10% and passive C reduced 10%; (2) slow C reduced 10% and passive C increased 10%.

^d(1) β increased 0.01; (2) β decreased 0.01.

^e(1) Clay fraction increased 10% and sand fraction decreased 10%; (2) clay fraction decreased 10% and sand fraction increased 10%.

[66] For simulations that include erosion or deposition, a biogeochemical model must have a realistic mechanism to account for the change of C content in each soil layer. By dynamically removing soil layers in the erosional cases or creating layers in the depositional cases, and using moisture, temperature, and aeration functions to determine decomposition rates, EDCM is able to simulate SOC changes in a soil profile. Figure 1 shows that the fraction of passive carbon at about 50 cm is higher in the MAXD case than in the other cases, reflecting the dynamic interaction between the deposition of subsoil materials with a relatively high proportion of passive C and the continued incorporation of new residue at the surface. We can also observe that the amounts of slow and passive C in the subsoil layers are considerably higher in the depositional cases than in the NOED or erosional cases. In Figure 5, panel C2, the curve for the MAXD case is above the curve for the MIND case by more than the MIND curve is above the NOED curve. This may be due to a reduced rate of decomposition at depth, as influenced by moisture, temperature, and aeration.

8.3. Comparison With CENTURY in the Topsoil Layer

[67] The fundamental difference between EDCM and its predecessor CENTURY is the number of soil layers used to simulate biogeochemical processes in the model. CENTURY

is designed to simulate carbon and nutrient dynamics in the top 20-cm layer. In contrast, EDCM adopts a multiple soil layer structure that enables the simulation of biogeochemical processes in the entire profile. Furthermore, the number of soil layers varies in EDCM during model simulations to dynamically account for the influences of soil erosion or deposition on the evolution of a soil profile.

[68] We compared our EDCM simulations of SOC dynamics in the top 20-cm layer to the simulations of *Harden et al.* [1999] using the CENTURY model (Figure 7). In making this comparison we used the original CENTURY IV data and model code that were employed and published on the internet by J. W. Harden et al. (<http://www.nrel.colostate.edu/projects/century/mississippi.htm>, and links cited therein). We observed several important differences.

[69] First, the steady state forest spin-up simulations of J. W. Harden et al. included a simulated fire and complete tree removal every 100 years. We performed CENTURY IV simulations using the Harden et al. code without these events, and determined that the resulting steady state SOC level was much higher than the observed field measurements. Harden et al. did not document their reasons for including fire and tree removal in their spin-up. We did not apply fire or tree removal events in the EDCM forest spin-up, yet EDCM yielded a steady state SOC concentration in reasonable agreement with observations. We conclude that

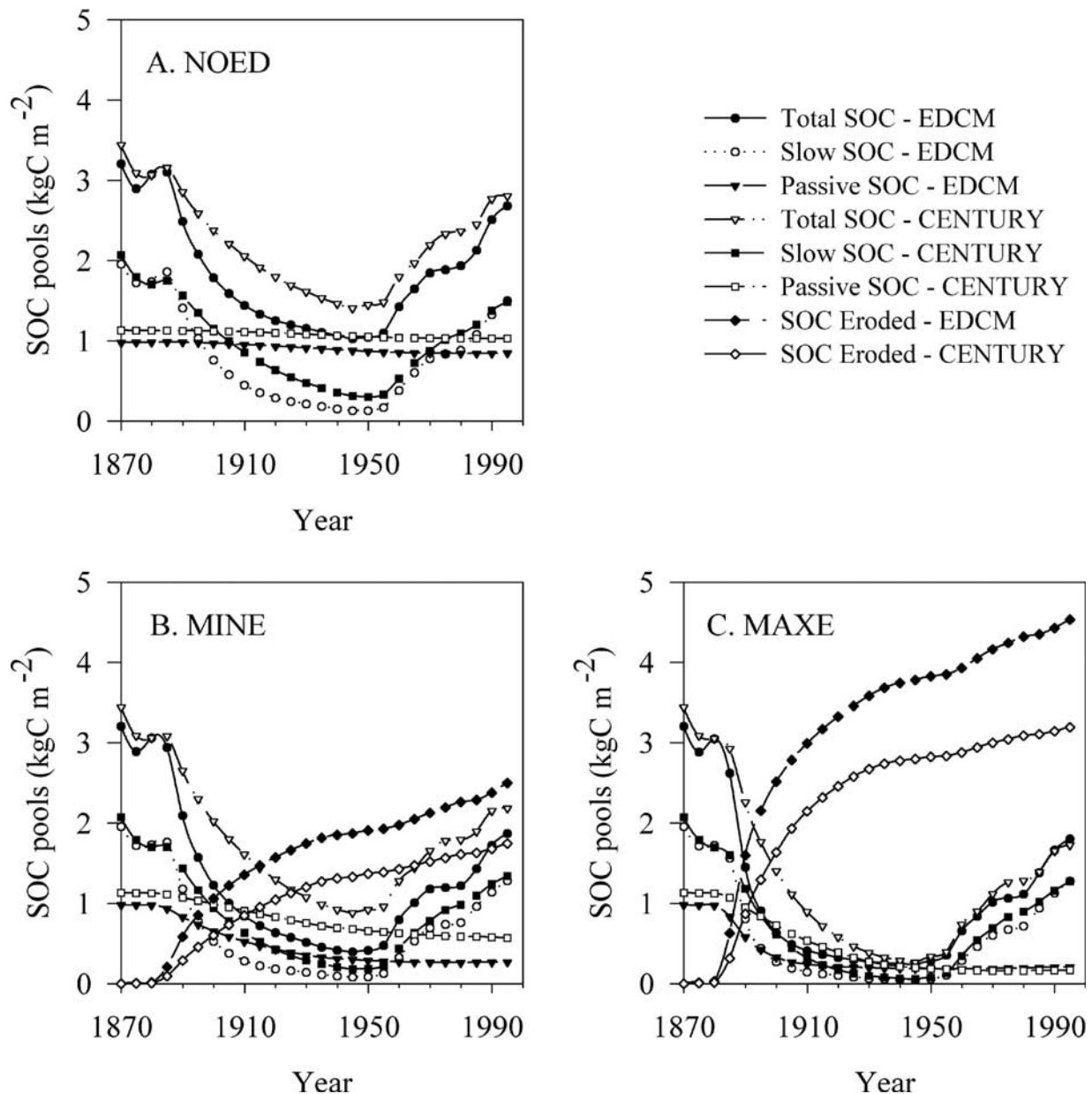


Figure 7. Comparison of the dynamics of total (somtc), slow (som2c), and passive (som3c) SOC in the top 20-cm layer, and eroded SOC simulated by EDCM and CENTURY under the control and two erosional scenarios. CENTURY simulations were from *Harden et al.* [1999].

EDCM and CENTURY IV differ fundamentally in their simulation of steady state forest SOC levels.

[70] Second, EDCM estimated soil depth reduction due to erosion ranging from 23 to 61 cm, as compared with an estimate of 15 to 20 cm from *Harden et al.* [1999]. We cannot explain the difference, but we note that *Harden et al.* reported that their estimated soil erosion from 1870 to 1997 resulted in a total loss of 340 to 869 kg soil m^{-2} . Assuming a reasonable bulk density of 1400 kg m^{-3} , this range of eroded soil mass would be equivalent to a depth of 22 to 62 cm, which is very close to our estimates.

[71] Another difference was that the total eroded SOC simulated by EDCM was much higher than that reported by *Harden et al.* [1999]. This difference appears to be caused by

several factors. The values used by *Harden et al.* to define the initial steady state values for the “subsoil” C pool were lower in the published code than those reported in their paper. Our experiments using the *Harden et al.* code indicate that the choice of values for these parameters has a more significant effect than reported by *Harden et al.* Their use of low initial subsoil SOC concentrations, and the passive depletion of SOC in their “subsoil” pool, meant that there was less SOC available for removal by erosion. In addition, differences in the enrichment factor (“enrich”) and model structure probably also contributed to this difference. On the basis of field observations [*Collins et al.*, 1997; *Starr et al.*, 2000], we used an enrichment factor of 2 in our study. In contrast, *Harden et al.* used a value of 1. Our dynamic

approach for simulating the SOC stock in deep layers as well as the transfer of SOC from dynamic subsurface layer to the top layer was fundamentally different from Harden et al.'s static "subsoil" C pool approach. These differences inevitably affect the amount of SOC erosion.

[72] SOC depletion was more pronounced in our study during the depletion period (1870 to 1950) for all landscape positions. Some of this difference might be caused by differences in NPP estimation, as suggested by the differences observed in control simulations without erosion or deposition (Figure 7a). Our NPP estimates were constrained by historical grain yield (Figure 4). A similar constraint was not used by *Harden et al.* [1999], possibly contributing to the slower depletion of SOC from 1870 to 1950 in that study. Although the trends of simulated SOC recovery after 1950 were similar in both models, the rate of soil carbon erosion continued to be higher in the EDCM simulations at all times.

[73] Finally, we were unable to reproduce *Harden et al.*'s [1999] offline calculation of the decomposition of eroded SOC for comparison to our EDCM depositional scenarios. We determined that the integrated soil carbon flux used in their offline calculations for net carbon exchange without erosion (their Figure 6) was much greater than the integrated flux calculated directly from their CENTURY IV model output. This observation calls into question the offline calculations of Harden et al. regarding effects of erosion on net carbon exchange. For similar reasons, we were unable to reproduce Harden et al.'s off-line calculation of radiocarbon levels in eroded soils. Thus the conclusions of *Harden et al.* [1999] regarding landscape-scale carbon balance appear to be limited by problems in their offline calculations, which were necessary because CENTURY IV is not capable of simulating the dynamic processes affecting SOC at sites of deposition.

[74] Because CENTURY only simulates SOC dynamics in the top layer, it is impossible to do similar comparisons for the deep layers or for the entire profile. From Figure 5 we can see that SOC dynamics in the deep layers and the whole profile were different from those in the top layer. Therefore, to evaluate the impacts of soil erosion and deposition on SOC storage and soil-atmospheric CO₂ exchange, a model with a multiple soil layer structure is required.

8.4. Impact of Soil Erosion and Deposition on Carbon Source or Sink

[75] Carbon sinks occur when there is a net flux of carbon from the atmosphere to the soil. Although a full budget for the influence of erosion and sedimentation on the carbon cycle awaits further work, elements of the budget at particular points on the landscape are observable in the simulations shown here. Equation (2) suggests that whether a soil is a net sink or source to atmospheric C depends on the difference between the rate of change of SOC and the rate of SOC erosion or deposition. The soil would be a net source at an erosional site if the rate of soil SOC decrease exceeded the SOC erosion rate. It would be a source in a depositional environment if the rate of increase in stock were less than the rate of C deposition. The soil would be a

net sink if the opposite relationships held. If the change in the carbon stock equaled the erosion or deposition rate, the soil would be neither a sink nor a source.

[76] Erosion reduces carbon emissions from the soil into the atmosphere during periods when the SOC is being depleted (e.g., from 1870 to 1950) (Table 4). There is less flux to the atmosphere because there is less SOC in the profile (a quantity change) and the SOC now at the surface has a higher proportion of passive SOC, a characteristic of its origin in the deep layers (a quality change). These changes in SOC quantity and quality tend to reduce the amount of CO₂ emissions from the soil into the atmosphere at sites of erosion. The erosional scenarios indicate enhanced C absorption since 1950, when SOC storage started to increase under the influences of improved management practices and intensified fertilization (Table 3). On the other hand, depositional sites are net C sources to the atmosphere. The C efflux tends to be higher than the rate of C absorption by photosynthesis at the depositional sites because of the additional oxidation of deposited SOC. These findings have not been reported previously. We present them as hypotheses for future testing using long-term field flux measurements [*Wofsy et al.*, 1993; *Baldocchi et al.*, 1996].

8.5. Toward a Landscape Model

[77] Although it is useful to study the separate impacts of erosion and deposition on SOC and C sources/sinks to gain insight into various processes, it is important to keep in mind that the overall budget of C between the soil and atmosphere should be assessed at a spatial scale that incorporates both erosion and deposition, such as a watershed. Our modeling study, as presented in this paper, is useful for investigating the dynamic nature of the SOC storage and the soil-atmospheric C exchange under the impact of soil erosion and deposition. However, a C mass balance could not be reached at the watershed scale because each run of the model applies to a small homogeneous patch of the landscape. Creating a C budget at the watershed scale will be the next step in model development, to completely account for the impacts of erosional, transport, and depositional processes on SOC dynamics and the soil-atmosphere C exchange.

[78] At the landscape scale, depositional soils can be expected to differ depending on the extent to which material eroded from a large area is focused into deposition in a relatively small area. Figure 8 shows the temporal changes of soil profile thickness, total SOC in the soil profiles, and cumulative CO₂ emissions from deep soil layers under two deposition scenarios. The first is the widespread deposition scenario (WDS) with a ratio of 1:1 (erosional area:depositional area). The other is the concentrated deposition scenario (CDS) with a ratio of 4:1 (erosional area:depositional area). Starting from 2 m, soil profile thickness reached 4.55 m under the CDS at the end of simulation, in contrast the thickness of soil profile only increased to 2.64 m under the WDS. SOC in the entire profile under CDS at the end of simulation reached 18,222 gC m⁻², equivalent to 582% and 222% of those under the MAXD and WDS scenarios, respectively. The total SOC in the WDS scenario increased 6656 gC m⁻² after adjustment by a factor of 4 for compar-

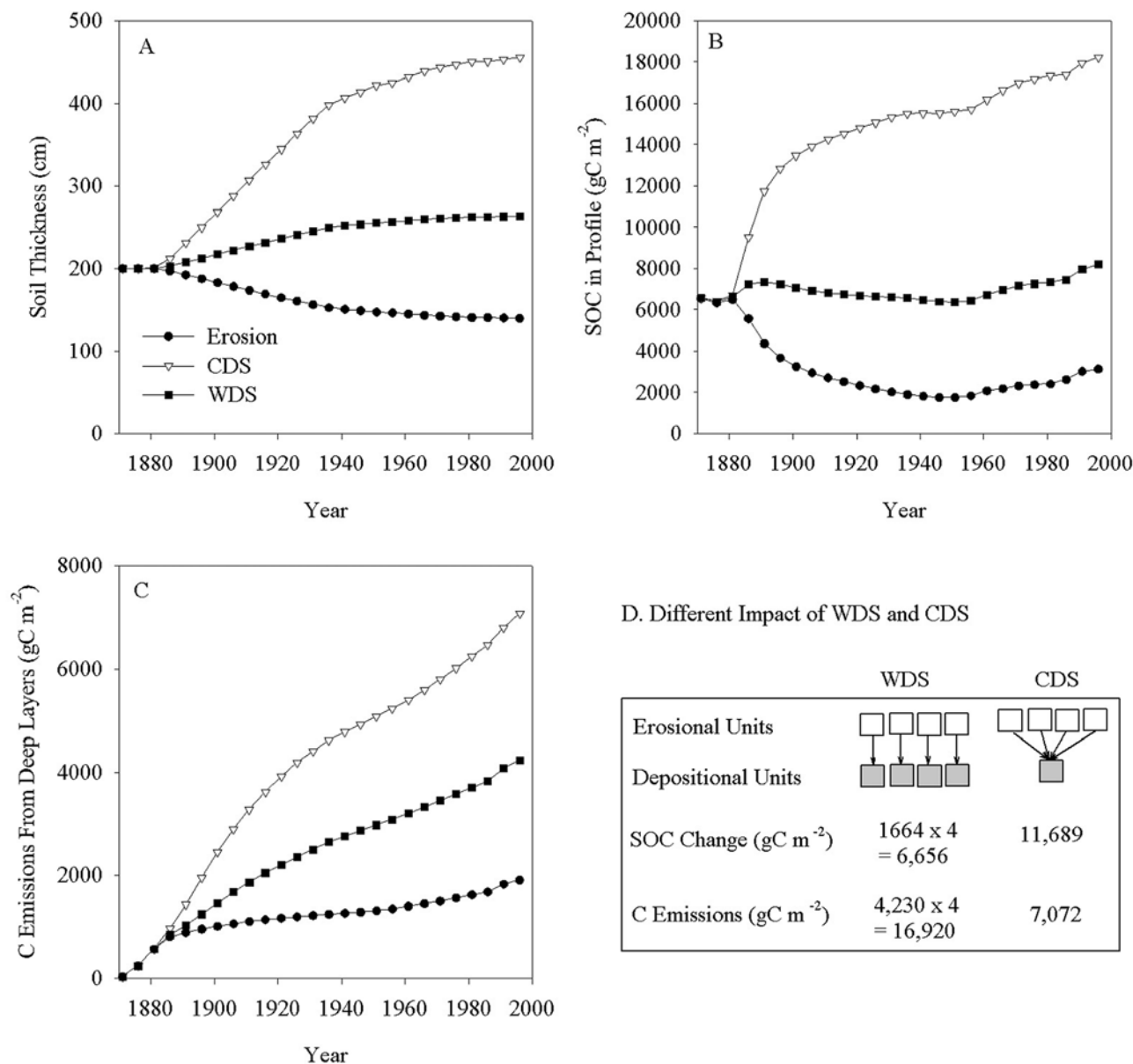


Figure 8. Impact of the ratio of erosional to depositional area on SOC dynamics. Two ratios are presented. The first is the 1:1 ratio, representing a widespread deposition scenario (WDS). The other is the 4:1 ratio, representing concentrated deposition scenario (CDS).

ison to the CDS scenario. This increase was significantly lower than the corresponding SOC increase of $11,689 \text{ gC m}^{-2}$ under CDS (Figure 8d). The area-adjusted cumulative CO_2 emissions from deep layers were $16,920 \text{ gC m}^{-2}$ and 7072 gC m^{-2} under WDS and CDS, respectively. Both SOC storage change and CO_2 emissions from deep layers indicated that concentrated deposition was more efficient in reducing CO_2 emissions from depositional sites. The results suggest that the redistribution patterns of eroded soil and SOC on the landscape has a significant impact on SOC dynamics.

[79] Although it is useful to study the separate impacts of erosion and deposition on SOC and C sources/sinks to gain

insight into various processes, it is important to keep in mind that the overall budget of C between the soil and atmosphere should be assessed at a spatial scale that incorporates both erosion and deposition, such as a watershed. Our modeling study, as presented in this paper, is useful for investigating the dynamic nature of the SOC storage and the soil-atmospheric C exchange under the impact of soil erosion and deposition. However, a C mass balance could not be reached at the watershed scale because each run of the model applies to a small homogeneous patch of the landscape. Creating a C budget at the watershed scale will be the next step in model development, to completely account for the impacts of erosional, transport, and deposi-

tional processes on SOC dynamics and the soil-atmosphere C exchange.

9. Conclusions

[80] The EDCM model has been developed to evaluate the impact of soil erosion and deposition on SOC storage and the C exchange between soil and the atmosphere. Traditionally, the change of SOC storage under the influences of erosion and deposition has been used to evaluate these impacts. Although this storage-based (or state-variable) approach is simple, straightforward, and easy to apply to field observations, it could not effectively reflect the dynamic interactions among the soil, atmosphere, and erosion and deposition. Our study shows that erosion has a negative impact on the SOC storage at eroding sites and deposition has a positive impact on the SOC storage at depositional areas compared with the sites that are identical but without erosion or deposition. In this study, we further assessed the impact of soil erosion and deposition on C sources and sinks and found important results that could not be revealed by using the state-variable approach.

[81] Soil erosion and deposition tend to reduce CO₂ emissions from the soil into the atmosphere by exposing low C soil at eroding sites and by burying high C soil at depositional sites. In addition to its status in croplands, eroded carbon buried in wetlands and water bodies can further contribute to reducing the rates of increase of atmospheric CO₂ [Stallard, 1998]. This effect may help to explain a part of the contemporary “missing sink” in the global carbon budget. However, to account for the overall impacts of soil erosion and deposition on carbon dynamics at watershed, regional, and global scales, we need a distributed approach that combines the carbon dynamics in the soil vertical profile with the accounting of sources and the fate of the eroded carbon on the landscape and water bodies.

[82] Our results suggest that erosion and deposition on croplands may result in lower atmospheric CO₂ levels than would have occurred with the same land use patterns without erosion and deposition. This does not necessarily mean that erosion and deposition are beneficial to the environment. Erosion and deposition decrease site fertility, contribute to nonpoint pollution, and reduce the efficiency and life expectancy of navigation systems and reservoirs. Our results suggest that failing to account for the impact of soil erosion and deposition may contribute to an overestimation of the total historical carbon released from soils because of land use change [Houghton *et al.*, 1999].

Appendix A

A1. Net Primary Production

A1.1. Modeling Approach

[83] Net primary production (NPP) is an important measure of the capability of an ecosystem to convert solar energy and atmospheric CO₂ to plant biomass. Because NPP has a significant impact on the storage and rates of change of organic carbon in vegetation and soil, the prediction of the temporal change of NPP is critical for the simulation of carbon dynamics for a given ecosystem. The NPP of a given site depends on many factors, including

potential primary productivity (PPP), nutrient and water availability, and management practices, such as planting density. PPP is the optimal primary productivity a system can reach without limitation from environmental variables such as nutrients, water, and radiation. Because the limiting factors change over time, so does NPP. In CENTURY, the carbon flux of net primary productivity $C_{NPP}(t)$ at time t is calculated from the carbon flux of potential primary productivity $C_{PPP}(t)$, with consideration of environmental limitations [Metherell *et al.*, 1993; Parton *et al.*, 1993],

$$C_{NPP}(t) = \zeta(t)C_{PPP}(t), \quad (A1)$$

where $\zeta(t)$ is a scaling factor varying between 0 and 1, representing the impacts of a collection of environmental variables, such as nutrients and water availability, on $C_{PPP}(t)$.

[84] To simulate the historical change in NPP using equation (A1), we have to specify PPP values for all the species or cultivars that were cultivated in the history of the site. This is a challenge for long-term simulations, considering that the PPP of a crop can change over time. Grain yield and harvest index have increased dramatically in the United States for almost every crop, but the rate of change of harvest index has been slower [Hay, 1995], indicating that NPP of different species must have changed as well. In EDCM, historical change of NPP is predicted by land use and land cover change data (specifically species shift) and by general patterns of grain yield and harvest index of crops using the following approach.

[85] The following relationship exists between $C_{NPP}(t)$ and grain yield:

$$C_{NPP}(t) = \frac{C_g(t)}{\omega(t)H_i(t)}, \quad (A2)$$

where $C_g(t)$ is the C in the grain, $\omega(t)$ is the ratio of aboveground biomass C to total biomass C at time t , and $H_i(t)$ is the harvest index (the ratio of grain biomass C to aboveground biomass C during harvest). According to equation (A2), the ratio of NPP at time t and time l can be expressed as

$$\frac{C_{NPP}(t)}{C_{NPP}(l)} = \frac{\omega(l) C_g(t) H_i(l)}{\omega(t) C_g(l) H_i(t)}. \quad (A3)$$

Assuming that $C_{PPP}(l)$ is given as input and combining equations (A1) and (A3), we can simulate the historical change of crop NPP using the historical patterns of grain yield and harvest index,

$$C_{NPP}(t) = \zeta(l) \frac{\omega(l) C_g(t) H_i(l)}{\omega(t) C_g(l) H_i(t)} C_{PPP}(l). \quad (A4)$$

A1.2. Historical Change of Crop Residue Production

[86] The rate of plant residue input is an important factor regulating net carbon fluxes into the soil and therefore the amount of SOC storage. Plant residue input depends on a variety of factors, including net primary productivity and harvesting practices, such as how much grain or straw is

removed from the site. In this study, we used the following procedures to estimate carbon input by means of plant residue into soils:

$$\begin{aligned} C_{\text{residue_input}}(t) &= C_{\text{NPP}}(t) - C_{\text{removed}}(t) \\ &= C_g(t)(1 - \alpha(t)) + C_a(t)(1 - \eta(t)) \\ &\quad + C_b(t)(1 - \tau(t)), \end{aligned} \quad (\text{A5})$$

with

$$C_a(t) = \left(\frac{1}{H_i(t)} - 1 \right) C_g(t) \quad (\text{A6})$$

$$C_b(t) = \left(\frac{1}{\omega(t)} - 1 \right) (C_g(t) + C_a(t)), \quad (\text{A7})$$

where t is time, C_g , C_a , and C_b are C in grain, aboveground nongrain biomass, and belowground biomass at time t , respectively, $\alpha(t)$, $\eta(t)$, and $\tau(t)$ are the fractions of C_g , C_a , and C_b being removed from the site at time t , respectively, $H_i(t)$ is the harvest index at time t , defined as $C_g(t)/(C_g(t) + C_a(t))$, and $\omega(t)$ is the ratio of aboveground biomass C to total biomass C at time t .

A2. Soil Carbon Decomposition

[87] Five SOC pools (i.e., metabolic, structural, fast, slow, and passive pools) in each soil layer are used in EDCM to characterize the quantity and quality of SOC, following the practice of CENTURY for the top layer [Parton *et al.*, 1987, 1993; Metherell *et al.*, 1993]. Soil and SOC movements between the top and the second layer are necessary to keep the thickness of the top layer fixed under erosion or deposition environments [Schimel *et al.*, 1985; Bouwman, 1989; Harden *et al.*, 1999]. Using five pools for each soil layer allows a tight coupling between the top and the second layer, and thus the exchange of SOC between these two layers can be quantified properly. The SOC dynamics in each of the layers were simulated as a result of the interactions of the following processes: erosion or deposition, litter input, decomposition, and leaching.

[88] In CENTURY, the decomposition of SOC in each pool i is calculated using the following equation:

$$\frac{dC_i(t)}{dt} = K_i L_c W(t) T(t) T_m C_i(t), \quad (\text{A8})$$

where $C_i(t)$ is the amount of C in pool i at time t , K_i is the maximum decomposition rate (yr^{-1}) for the SOC in pool i , $W(t)$ and $T(t)$ are the impacts of soil moisture and soil temperature on decomposition at time t , T_m is the effect of soil texture on SOC turnover, and L_c is the impact of the lignin content of structural material on structural decomposition. A detailed description of the definitions of these parameters, along with methods for quantifying carbon flows among various pools, microbial respiration, and leaching, are given by Metherell *et al.* [1993].

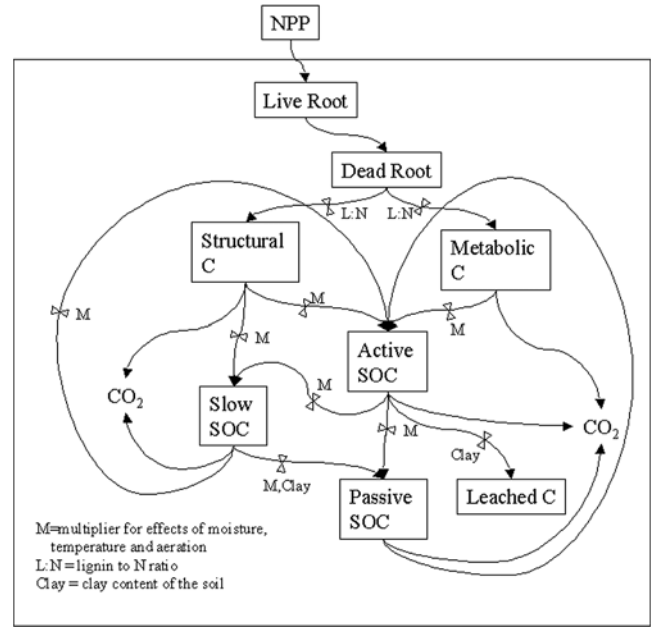


Figure A1. Transformation and decomposition of soil organic carbon within deep soil layers are affected by soil moisture, temperature, aeration, texture, and quantity and quality of litter input.

[89] In EDCM, we extended equation (A8) to predict the decomposition of SOC in various pools in deep layers (see Figure A1):

$$\frac{dC_i(z, t)}{dt} = K_i L_c W(z, t) T(z, t) T_m(z) A(z) C_i(z, t), \quad (\text{A9})$$

where z is soil depth, and $A(z)$ is the degree of aeration at depth z . The logic to add $A(z)$ into equation (A9) was based on the observation that decreased aeration in deep layers leads to reduced SOC decomposition [Van Dam *et al.*, 1997]. In the following subsections, the methods for simulating soil moisture and temperature and their impacts on SOC decomposition, as well as the form of $A(z)$, are presented. The algorithms for determining other parameters in equation (A9) are inherited from CENTURY [Metherell *et al.*, 1993; Parton *et al.*, 1993] and are not described here.

A2.1. Hydrological Submodel and the Impact of Soil Moisture on Decomposition

A2.1.1. Hydrological Submodel

[90] For the simulation of plant growth and SOC decomposition, it is necessary to predict the temporal change of soil moisture in the soil profile. The hydrological processes as represented in the hydrological submodel of CENTURY are oversimplified. CENTURY assumes that total monthly precipitation occurs in a single event with the soil being wetted once. The change in soil moisture content is calculated using the difference between rainfall and potential evapotranspiration (PET). If the difference is larger than the field capacity of the soil, soil moisture is set equal to field capacity; and the rest of the difference goes to runoff or deep percolation. If the difference is nonpositive (i.e., PET

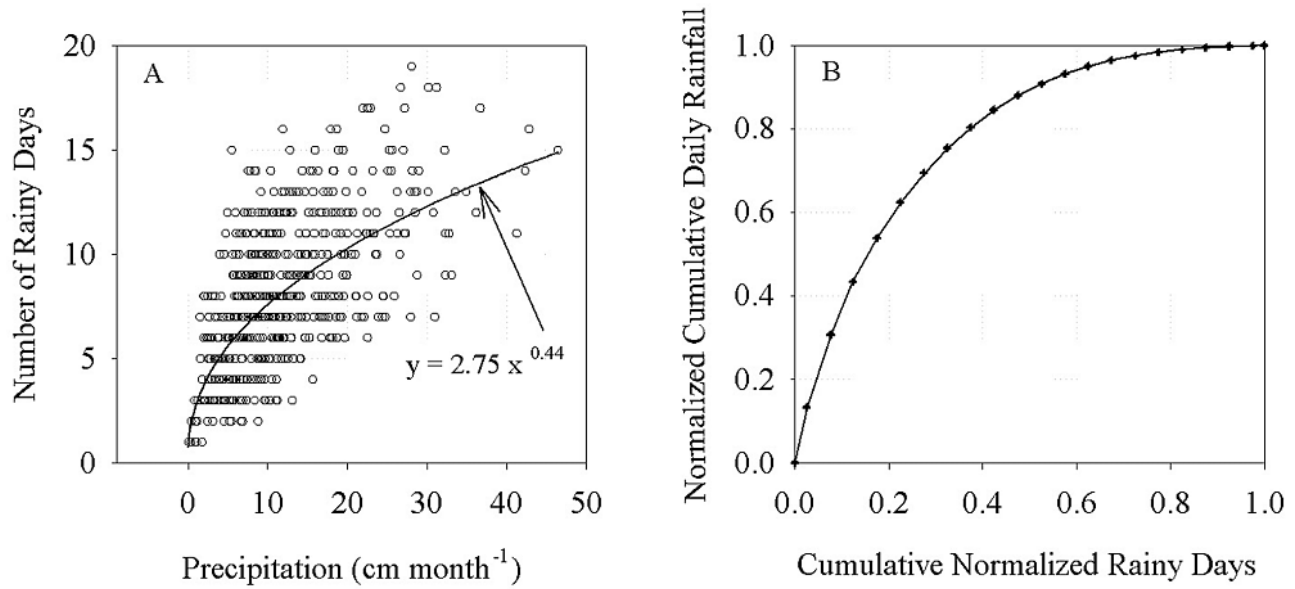


Figure A2. (a) Relationship between monthly precipitation and the number of rain days and (b) distribution of normalized cumulative daily rainfall as observed in Batesville, Mississippi, from 1948 to 1997. Daily rainfall was sorted in descending order in Figure A2b, which shows that more than 80% of the rainfall occurred on 40% of the rainy days in the region.

is not smaller than rainfall), evapotranspiration depletes the available soil water until either the PET requirement is met or the soil moisture content reaches the wilting point of the soil. When this scheme is used, the soil moisture content often remains at field capacity in areas with abundant rainfall and reaches the wilting point in areas where PET is larger than rainfall.

[91] A new hydrological submodel has been developed in EDCM to replace the original CENTURY version. The basic concept of the hydrological submodel is based on work by Liu *et al.* [2000], but there are several important modifications. The new model uses statistical relationships to estimate the number of rainy days in a month and then allocate the total monthly rainfall to each rainy day. Monthly rainy days can be estimated from monthly rainfall using the relationship between monthly precipitation and rainy days. This relationship can be derived from historical daily rainfall information. For example, Figure A2 shows that monthly rainy days increase nonlinearly with the amount of monthly precipitation at Batesville, Mississippi. Such a relationship can be found in other regions as well (e.g., in a tropical rainforest climate [Liu *et al.*, 2000]). In EDCM, we use the long-term distribution of daily rainfall to allocate monthly precipitation to each individual rainy day in the month. The long-term distribution of daily rainfall can be derived using the following procedures:

[92] 1. Sort all daily rainfall values in descending order. The daily rainfall data should at least cover 1 year of observations.

[93] 2. Using the sorted list of daily rainfall values, calculate relative cumulative rainy days (Rd). A relative rainy day is $1/N$, where N is the total rainy days.

[94] 3. Calculate relative cumulative daily rainfall (Rr). Relative daily rainfall is daily rainfall divided by total rainfall.

[95] 4. Develop the normalized composition curve of daily rainfall: $Rr = f(Rd)$. In most cases, this function is nonlinear, indicating that the distribution of different classes of daily rainfall is not even. For example, Figure A2b shows that more than half of the precipitation occurs in 20% of the rainy days, while the other 40 ~ 50% of the precipitation falls on 80% of the rainy days.

[96] Let the monthly rainy days be m (as estimated from monthly precipitation), and the rainfall amount for rainy day i in EDCM is estimated from the following formula:

$$R_i = R \left(f\left(\frac{i}{m}\right) - f\left(\frac{i-1}{m}\right) \right), \quad (\text{A10})$$

where $i = 1, 2, \dots, m$, R_i and R are the daily and monthly precipitation, respectively. In the above formula, we implicitly assumed that the daily rainfall amounts of these m rainy days follow the long-term statistical relationship as defined by the $Rr = f(Rd)$ function. Note that actual daily precipitation may show randomness in reality and seldom follow the curve $Rr = f(Rd)$ exactly. But in the long run, we expect actual daily precipitation would follow the curve statistically. In EDCM, the sequencing (or relative positions) of these rainy days and the interval between consecutive rainy days are assumed to follow random distributions.

[97] Each daily net rainfall (i.e., gross daily rainfall R_i minus interception) was routed through the topsoil layer by simply filling up soil moisture content, and any excess over the field capacity was routed through the lower layers. No

soil hydraulic properties were used in routing owing to the coarse time step used in the model. The monthly evapotranspiration rate was estimated by the algorithms in CENTURY, which is a modified version of the Penman-Monteith approach [VEMAP Members, 1995]. The vertical distribution of evapotranspiration was assumed to be proportional to the root distribution in the soil. The monthly soil moisture content for each layer was calculated as the mean of moisture contents at the beginning and end of the month for the layer. The moisture content at the end of the month was estimated on the basis of the moisture content at the beginning of the month and on inputs (precipitation or routed water from the upper layer) and outputs (evapotranspiration and deep percolation) during the month.

[98] To quantify the amounts of available water for plant growth and survival, CENTURY adopted a scheme with multiple soil layers for its hydrological simulation. Two parameters, NLAYER and NLAYPG, were used to specify the number of layers for calculating the amount of soil water for survival and for growth, respectively. These parameters were considered as site specific and not really associated with individual plant species or plant functional type [Metherell *et al.*, 1993]. However, in reality, they may change following the change of species on a given site. If a deep-rooted species were replaced by a shallow-rooted species, the amounts of available water for plant survival and growth would be overestimated if these parameters were not reduced accordingly [Fisher *et al.*, 1994]. In EDCM, NLAYER and NLAYPG are explicitly associated with a plant species and defined by its rooting characteristics. NLAYPG and NLAYER are calculated from the depths at which the cumulative roots reach 95% and 98% of the total root biomass, respectively. Consequently, EDCM is capable of dynamically adjusting these parameters to reflect the change of rooting properties following land cover change.

A2.1.2. Impact of Soil Moisture Content on Decomposition

[99] Previous studies have suggested that there is an optimal soil moisture content for C and N mineralization [Lin and Doran, 1984; Skopp *et al.*, 1990; Howard and Howard, 1993]. If soil moisture is below the optimum, soil microbial activities are restricted and increase monotonically with soil moisture content. When soil moisture exceeds the optimum, anaerobiosis prevails and soil microbial activities are reduced because of oxygen limitation. On the basis of these observations, the impact of soil moisture on SOC decomposition in EDCM is calculated as

$$W(z, t) = \begin{cases} \max\left(w_l, \frac{v(z, t)}{v_0}\right) & \text{if } v(z, t) < v_0 \\ \max\left(w_l, 1 - \frac{1 - w_l}{1 - v_0}(v(z, t) - v_0)\right) & \text{if } v(z, t) \geq v_0 \end{cases}, \quad (\text{A11})$$

where $v(z, t)$ is the fraction of water-filled pore space (WFPS) in soil layer z , v_0 is the optimum WFPS value for microbial activities, and w_l is the minimum impact of soil moisture on decomposition. Many studies have shown that v_0 varies around 0.75 [Lin and Doran, 1984].

A2.2. Impact of Soil Temperature

[100] The algorithms used in CENTURY for calculating soil temperature of the top layer [Parton, 1984] and the impact of soil temperature on SOC decomposition [Parton *et al.*, 1987, 1993] are retained in EDCM. Here only the methods for predicting soil temperature in deep layers are described.

[101] The seasonal change of soil temperature at deeper soil layers was simulated using a harmonic relationship [Hillel, 1980], normalized by the soil temperature of the surface layer as predicted by the original CENTURY treatment. CENTURY simulates soil temperature as a function of air temperature, aboveground biomass, and soil properties [Parton, 1984]. The combination of the CENTURY method with the method described below provides a new way to simulate not only the seasonal harmonic pattern but also the monthly irregular fluctuations of soil temperature at different depths caused by fluctuations of air temperature.

[102] According to Hillel [1980], the annual variation of soil temperature at various soil depths can be expressed by

$$T(z, t) = \bar{T}(z) + \frac{A(0)}{e^{z/d_m}} \left[\sin\left(\omega t + \varphi - \frac{z}{d_m}\right) \right], \quad (\text{A12})$$

where z is soil depth, t is time, $T(z, t)$ is soil temperature at depth z and time t , $\bar{T}(z)$ is annual mean temperature at depth z , ω is radial frequency ($= 2\pi/p$, p is the time interval, $\omega = 1.99 \times 10^{-7} \text{ (s}^{-1}\text{)}$ for an annual variation), φ is a phase constant, and d_m is a damping depth, at which the temperature amplitude decreases to the fraction $1/e$ ($1/2.718 = 0.37$) of the temperature fluctuation (the range from the maximum to the mean temperature) at the soil surface $A(0)$.

[103] The damping depth is related to the thermal properties of the soil and the frequency of the temperature fluctuation, as follows [Hillel, 1980]:

$$d_m = \sqrt{\frac{2\kappa}{H_c\omega}} = \sqrt{\frac{2D}{\omega}}, \quad (\text{A13})$$

where κ is thermal conductivity of the soil, H_c is volumetric heat capacity of a soil, and D is thermal diffusivity. The above three parameters (i.e., κ , H_c , and D) define the thermal properties of the soil. Thermal conductivity was calculated using soil bulk density and volumetric water content following Yin and Arp [1993]. The heat capacity of a soil equals the sum of the heat capacities of different constituents [Fairbridge and Finkl, 1979]:

$$H_c = 0.48f_{\text{solids}} + f_{\text{water}} + 0.6f_{\text{SOM}}, \quad (\text{A14})$$

where 0.48, 1, and 0.6 are the heat capacities of constituent soil solids, water, and soil organic matter with a volume fraction f_{solids} , f_{water} , and f_{SOM} , respectively. The air content and its addition to the soil's H_c are ignored in equation (A14) owing to its very low heat capacity, although differences in air-filled porosity will affect H_c indirectly by affecting the other volume fractions.

A2.3. Impact of Soil Aeration

[104] Soil moisture is closely related to soil aeration. Expecting that the impact of soil aeration on SOC decom-

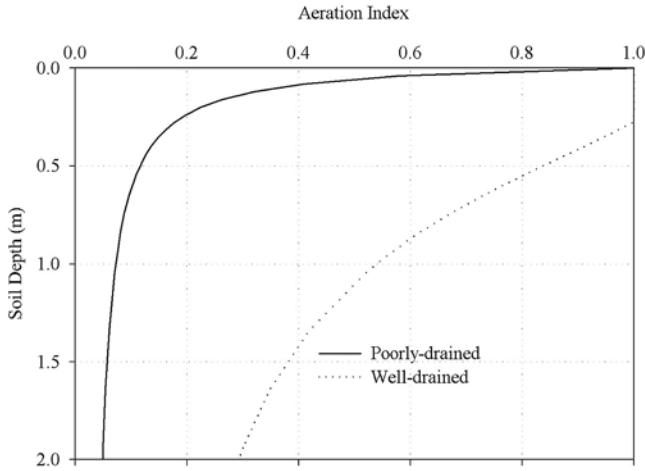


Figure A3. Hypothetical relationship between soil aeration and soil depth.

position might be adequately represented by soil moisture, we initially ran the model without explicitly considering the impact of aeration on SOC decomposition in soil profiles. Results suggested that moisture by itself was insufficient to account for what is observed in the vertical distribution of SOC. We concluded that an aeration term is needed for simulating the SOC dynamics in soil profiles.

[105] The impact of soil aeration on mineralization has been studied near the soil surface [Renault and Sierra, 1994; Li et al., 2000] or within the soil [Renault and Stengel, 1994]. The aeration in any deep layer is more complex because soil moisture contents in both this layer and its upper layers are important determinants. To our knowledge, no effective physically based description of the dynamics of soil aeration has been proposed. However, several studies directly [Van Dam et al., 1997] or indirectly [Voroney et al., 1981; Bouwman, 1989] indicated that SOC decomposition in deep layers is slower than could be explained by soil moisture, temperature, and soil texture, which are usually sufficient for the prediction of SOC dynamics in the surface layer. Soil moisture and temperature are not enough to explain the change of SOC turnover rates in soil profiles as observed in forests and pastures [Van Dam et al., 1997]. Slower turnover at depth was attributed by Van Dam et al. to a lower diffusion efficiency in the deep layers, and they suggested a diffusion factor for the purpose of modeling. To match simulated SOC profiles with field measurements, Van Veen and Paul [1981] and others [Voroney et al., 1981; Bouwman, 1989] applied further reduction factors of 0.8 and 0.6, respectively, to the temperature scaling factors of the second (15–40 cm) and third (40–80 cm) layers in their carbon turnover model. However, there does not appear to be a mechanistic justification for applying various additional reduction factors to the temperature effect in deep soil layers. In EDCM, we hypothesize that soil aeration decreases with soil depth and we model its effect on decomposition using an aeration factor analogous to other factors included in the CENTURY treatment of decomposition. This approach is based on the assumption that the diffusion of oxygen to deep layers

becomes increasingly difficult as depth increases. The following equation is used to describe the general vertical distribution of the soil aeration factor:

$$A(z) = \frac{1}{(1 + a \times e^{bz})^c} + f, \quad (\text{A15})$$

where a , b , c , and f are empirical coefficients used to define the specific shape of the vertical distribution of the aeration factor. Figure A3 presents two possible soil aeration factor profiles. Although $A(z)$ as defined by equation (A15) cannot be used to describe the dynamic nature of aeration changes in soil profile (as affected by soil moisture and bulk density fluctuations), we believe that this treatment is sufficient to describe the general pattern of aeration change with soil depth.

A3. Dynamic Accounting of Mass in Each Layer

[106] To keep the thickness of the top layer constant during erosion, the EDCM model transfers a certain amount of soil to the top layer from the second layer to account for the reduction of thickness caused by erosion. The procedure described below is similar to the scheme proposed in a number of studies [Schimel et al., 1985; Bouwman, 1989; Harden et al., 1999]. The amount of soil transferred is calculated as the eroded thickness multiplied by the bulk density of the second layer. This implicitly references a soil volume with a surface projection of 1 m². The transfer of SOC from deep layers (EDCM may need to transfer soil from the third layer, and so on, if the thickness of successive subsoil layers is less than the cumulative soil thickness eroded) to the top layer is performed separately for various pools according to the following:

$$\Delta C(1, i) = \sum_{j=2}^n C(j, i) * h_j, \quad (\text{A16})$$

where n is the number of the layer when the addition of its thickness, starting from the second layer, makes the cumulative thickness first exceed the thickness of the eroded soil, $\Delta C(1, i)$ is the cumulative amount of C in pool i that is transferred from the deep layers ($j = 2, \dots, n$) to the top layer ($j = 1$), $C(j, i)$ is the C in pool i layer j , and h_j is a coefficient defining the fraction of $C(j, i)$ being transferred to the top layer from layer j :

$$h_j = \begin{cases} 1 & \text{if } j < n \\ d_e - \sum_{m=2}^{n-1} d_m & \text{if } j = n, \end{cases} \quad (\text{A17})$$

where d_e is the thickness of eroded soil, d_m is the thickness of layer m , and d_n is the thickness of the n th layer. Soil properties in the top layer, such as bulk density and root biomass, were adjusted accordingly using a thickness-weighted approach. For example, the bulk density is calculated as

$$B_1 = \left(\frac{20 - d_e}{20} \right) B_0 + \sum_{j=2}^n h_j \frac{d_j}{20} B_j, \quad (\text{A18})$$

Table A1. Sensitivity of Some of the Output Variables to Input Variables as Represented by the EDCM Model Under the Minimum Deposition Scenario^a

Variable	Change, %	NPP ^b	Grain, gC m ⁻²	Straw, gC m ⁻²	C Depos.	Depth, cm	SOC in Profile, gC m ⁻²			SOC in Top 20 cm, gC m ⁻²			Cumulative Gross CO ₂ Emission, gC m ⁻²	
							Total	Slow	Passive	Total	Slow	Passive	0–20 cm	Deep Layers
Baseline (MIND)		190	3556	1906	2452	222.8	7023	2622	4015	2933	1753	813	16283	3261
Initial SOC	10	0.5	0.1	0.8	6.2	0.0	6.3	2.1	9.6	2.8	0.4	8.9	1.7	4.4
	-10	-0.5	-0.1	-0.8	-6.2	0.0	-6.3	-2.1	-9.6	-2.7	-0.4	-8.9	-1.8	-4.5
Initial SOC quality ^c	(1)	0.0	-0.1	-0.3	-6.6	0.0	-6.3	1.3	-11.8	-4.7	-0.1	-16.7	1.0	2.8
	(2)	0.0	0.0	0.2	5.1	0.0	5.0	-1.4	9.6	3.9	0.2	13.7	-1.2	-3.2
Soil deposition	10	-1.6	-0.2	-3.4	6.0	1.0	0.4	-0.9	1.4	-2.7	-2.0	-4.4	-1.1	1.1
	-10	0.0	-0.7	3.5	-6.6	-1.0	-2.3	-3.7	-1.6	-1.0	-3.7	4.2	0.4	-2.5
SOC deposition	10	0.5	0.1	0.7	10.0	0.0	1.8	1.0	2.4	2.5	1.3	6.2	0.8	0.7
	-10	0.0	-0.1	-0.7	-10.0	0.0	-1.8	-1.1	-2.4	-2.5	-1.3	-6.2	-0.8	-0.8
PPP	10	10.0	10.6	7.5	5.3	0.0	4.4	2.3	0.5	9.0	11.5	1.6	8.3	6.1
	-10	-12.6	-10.2	-8.0	-4.8	0.0	-4.5	-9.1	-0.6	-8.8	-11.1	-1.6	-10.9	-10.5
β (roots) ^d	(1)	5.8	3.5	2.5	3.7	0.0	2.0	4.1	0.4	1.9	2.1	0.7	3.4	17.3
	(2)	-8.4	-5.7	-8.4	-4.9	0.0	-3.3	-7.3	-0.5	-4.8	-6.5	-1.4	-5.7	-14.8
Aeration inde	10	0.0	0.0	-0.1	-0.2	0.0	-1.2	-2.1	-0.6	0.0	-0.1	-0.1	0.0	2.5
	-10	0.0	0.0	0.1	0.4	0.0	1.5	2.7	0.8	0.1	0.0	0.2	0.0	-3.1
Clay ^e	(1)	-0.5	-1.0	-0.7	0.1	0.0	0.6	0.9	0.5	-0.2	-0.7	0.9	-0.6	-1.6
	(2)	1.1	1.0	0.7	0.0	0.0	-0.5	-0.8	-0.5	0.3	0.7	-0.9	0.6	1.5
Bulk density	10	-3.2	-4.8	0.6	-6.3	0.0	2.2	6.8	-0.6	-1.7	-4.6	4.1	-2.5	-13.6
	-10	1.6	3.3	-0.3	7.7	0.0	-2.4	-7.4	0.6	-2.0	-1.0	-5.0	1.7	10.0
Temperature	5	-6.3	-10.8	-4.0	-2.6	0.0	-4.5	-9.3	-0.5	-8.6	-11.0	-1.2	-4.9	-0.6
	-5	5.8	9.5	3.8	1.7	0.0	4.0	8.2	0.4	7.4	9.2	1.2	4.2	0.2
Precipitation	5	2.1	3.8	1.7	0.4	0.0	0.1	0.5	0.0	0.1	0.5	0.0	1.9	0.0
	-5	-1.1	-1.9	-1.6	-0.1	0.0	0.4	1.1	0.0	0.9	1.5	0.2	-1.2	0.1

^aAll values except for the baseline are percentage change on the basis of the baseline scenario.

^bNPP is the average net primary productivity from 1870 to 1997 in gC m⁻² yr⁻¹; the following variables were expressed as cumulative during the simulation period: grain and straw harvested, C eroded and CO₂ effluxes; soil depth, total, slow, and passive SOC represented the values at the end of the simulation.

^c(1) slow C increased 10% and passive C reduced 10%; (2) slow C reduced 10% and passive C increased 10%.

^d(1) β increased 0.01; (2) β decreased 0.01.

^e(1) Clay fraction increased 10% and sand fraction decreased 10%; (2) clay fraction decreased 10% and sand fraction increased 10%.

where 20 is the thickness of the top layer in cm, B_0 is the bulk density of the top layer before erosion has taken place, B_1 is the bulk density of the top layer after erosion and soil replacement from the deep layers, and B_j is the bulk density of layer j ($j = 2, \dots, n$).

[107] Both erosion and deposition events are specified in the event schedule file using the flag EROD. The program determines if the event specified is erosion or deposition by looking at the sign of the rate that follows the flag. A positive value represents erosion (following CENTURY tradition), and a negative value represents deposition (a new addition to EDCM). The schedule file at a deposition site can be generated manually. Alternatively, a subroutine has been developed in EDCM to allow users to generate a schedule file from the output generated from an erosion site. This linkage provides a seamless connection between erosional source materials and depositional sites, and can be useful for developing a distributed model in the future.

A4. Sensitivity Analysis

[108] A sensitivity analysis was done to understand how selected model parameters influence the model results. Under erosion, a 10% increase of initial SOC leads to a 6.2% increase of SOC loss through erosion, 5.4% increase of SOC in the profile, and 4.8% increase of cumulative gross CO₂ efflux from deep soil layers (Table 5). The reason

a 10% increase did not introduce a 10% increase in eroded C was the oxidation of SOC during the course of simulation. Because of the very slow turnover of passive SOC, it is sensitive to the initial SOC. Of course, the passive SOC in the top layer should not be interpreted literally because the original top layer is lost by erosion during the simulation. Decreasing initial SOC would decrease SOC loss through erosion, SOC content in the profile, and cumulative gross CO₂ efflux from deep soil layers (Table 5).

[109] The quality of the initial SOC was also important to C eroded, passive C, and to a lesser degree, CO₂ efflux from deep layers. The C eroded and passive SOC at the end were more an indication of the amount of initial passive C because of its very large turnover time, while CO₂ efflux from deep layers was more sensitive to the initial slow SOC because of its relatively shorter turnover time. The rate of soil erosion had the strongest influence on the amount of C eroded, followed by the amount of passive SOC.

[110] Increasing potential primary production (PPP) by 10% leads to an increase in NPP (9.6%), grain yield (9.4%), straw harvest (6.4%), SOC erosion (5.3%), SOC in the profile (4.7%) and in the top layer (9.5%), and CO₂ effluxes from the top layer (8.4%) and deep layers (6.3%). SOC response to PPP was primarily caused by the high sensitivity of slow SOC to PPP. Passive SOC has little response to a change in PPP. Reducing PPP has the opposite impact of

increasing PPP. The high sensitivity of the EDCM to PPP justifies our effort and our emphasis on calibrating the model with historical grain yield data.

[111] Distributing more roots in deep layers and increasing rooting depth lead to an increase of NPP. This is tested by increasing the β factor in $y = 1 - \beta^z$, where y is the cumulative root fraction from the soil surface to depth z (in centimeters), from Jackson *et al.* [1996]. The NPP increase is probably caused by an increase in soil water available for plant growth owing to the increased rooting depth. With increased NPP and increased allocation of NPP to deep layers, the CO₂ efflux from deep layers increased by 25.4%, while at the same time SOC in the profile increased as well. Decreasing the rooting β factor has the opposite effect.

[112] For the site conditions at Nelson Farm, the EDCM is not very sensitive to the aeration index that describes the decreasing pattern of aeration in the soil profile as soil depth increases. A 10% increase in the aeration index leads to a 2.6% increase in the CO₂ emissions from deep layers. Decreasing the index leads to a 3.2% reduction in the emissions from the deep layers.

[113] An increase of 10% in the enrichment factor of the eroded soil translated into a 5.4% increase in SOC erosion and 10.3% decrease of passive C in the top layer. A higher enrichment factor means more SOC is eroded for a given soil erosion rate. Slow SOC can be replaced relatively easily by the decomposition of plant residue, and the replacement of passive C is difficult because of its slow turnover. Decreasing the enrichment factor has the opposite impact.

[114] The EDCM is not very sensitive to soil texture at this rather sandy site. However, it is sensitive to bulk density. Increasing bulk density leads to a reduction in NPP, grain yield, SOC erosion, and CO₂ effluxes. At the same time, SOC increases. In EDCM, bulk density affects NPP and SOC through its impact on water-holding capacity and heat capacity, which in turn affect the seasonal dynamics of soil moisture content and soil temperature. The increase in SOC could be attributed to decreased SOC oxidation, as indicated by reduced CO₂ effluxes.

[115] Increasing air temperature by 5% (which corresponds to an increase of 1.25°C on a base of 25°C during the growing season) leads to a reduction in production, SOC, and cumulative CO₂ effluxes. It is likely that 25°C is above the optimal temperature for NPP for most plants and that further increases in temperature would lead to a reduction in NPP. Decreasing the temperature parameter increases NPP and SOC.

[116] The EDCM is not very sensitive to precipitation in the region; presumably, precipitation is not a limiting factor for plant production. The sensitivity of EDCM on the depositional case MIND was roughly similar to its sensitivity on the erosional case MINE, with some differences in magnitude (Table A1). An increase in SOC deposition is an increase in the carbon content of the deposited materials, and it increases the passive pool in the surface layer. The influence of the rooting β factor on CO₂ emission from deep layers is not quite as strong as in the erosional case.

[117] **Acknowledgments.** This paper benefited from the constructive comments of several anonymous reviewers. This study was a part of the Mississippi Basin Carbon Project, which is supported by the U.S. Geolog-

ical Survey Global Change Research Program. Part of the work (S. L. and N. B.) was performed under U.S. Geological Survey contracts 1434-CR-97-CN-40274 and 03CRCN001.

References

- Austin, R. B., J. Bingham, R. D. Blackwell, L. T. Evans, M. A. Ford, C. L. Morgan, and M. Taylor, Genetic improvements in winter wheat yields since 1900 and associated physiological changes, *J. Agric. Sci. Cambridge*, *94*, 675–689, 1980.
- Baldocchi, D., R. Valentine, and S. Running, Strategies for measuring and modeling carbon dioxide and water vapor fluxes over terrestrial ecosystems, *Global Change Biol.*, *2*, 159–169, 1996.
- Bouwman, A. F., Modeling soil organic matter decomposition and rainfall erosion in two tropical soils after forest clearing for permanent agriculture, *Land Degrad. Rehabil.*, *1*, 125–140, 1989.
- Buyanovsky, G. A., and G. H. Wagner, Post-harvest residue input into cropland, *Plant Soil*, *93*, 57–67, 1986.
- Buyanovsky, G. A., and G. H. Wagner, Carbon cycling in cultivated land and its global significance, *Global Change Biol.*, *4*, 131–141, 1998a.
- Buyanovsky, G. A., and G. H. Wagner, Changing role of cultivated land in the global carbon cycle, *Biol. Fertil. Soils*, *27*, 242–245, 1998b.
- Chen, W., J. Chen, and J. Cihlar, An integrated terrestrial ecosystem carbon-budget model based on changes in disturbance, climate, and atmospheric chemistry, *Ecol. Modell.*, *135*, 55–79, 2000.
- Cihacek, L. J., and J. B. Swan, Effects of erosion on soil chemical properties in the north central region of the United States, *J. Soil Water Conserv.*, *49*, 259–265, 1994.
- Collins, A. L., D. E. Walling, and G. J. L. Leeks, Source type ascription for fluvial suspended sediment based on a quantitative composite fingerprinting technique, *Catena*, *29*, 1–27, 1997.
- Cox, T. S., J. P. Shroyer, B. Liu, R. G. Sears, and T. J. Martin, Genetic improvement in agronomic traits of hard red winter wheat cultivars from 1917 to 1987, *Crop Sci.*, *28*, 756–760, 1988.
- DeFries, R. S., L. Bounoua, C. B. Field, I. Fung, and G. J. Collatz, Combining satellite data and biogeochemical models to estimate global effects of human-induced land cover change on carbon emissions and primary productivity, *Global Biogeochem. Cycles*, *13*, 803–815, 1999.
- Donigian, A. S. Jr., T. O. Barnwell, R. B. Jackson, A. S. Partwardhan, K. B. Weinreich, A. L. Rowell, R. V. Chinnaswamy, and C. V. Cole, Assessment of alternative management practices and policies affecting soil carbon in agroecosystems of central United States, *EPA/600/R-94/067*, U.S. Environ. Prot. Agency, Athens, Georgia, 1994.
- Fairbridge, R. W., and C. W. Finkl Jr., *The Encyclopedia of Soil Science*, part 1, *Physics, Chemistry, Biology, Fertility, and Technology*, 646 pp., Dowden, Hutchinson and Ross, Stroudsburg, Pa., 1979.
- Fisher, M. J., et al., Carbon storage by introduced deep-rooted grasses in the South American savannas, *Nature*, *371*, 236–238, 1994.
- Frye, W. W., S. L. Elberhar, L. W. Murdoch, and R. L. Blevins, Soil erosion effects on properties and productivity of two Kentucky soils, *Soil Sci. Soc. Am. J.*, *46*, 1051–1055, 1982.
- Geng, G. Q., and D. R. Coote, The residual effect of soil loss on the chemical and physical quality of three soils, *Geoderma*, *48*, 415–429, 1991.
- Hadas, A., A. Feigin, S. Feigenbaum, and R. Portnoy, Nitrogen mineralization in the field at various soil depths, *J. Soil Sci.*, *40*, 131–137, 1989.
- Harden, J. W., T. L. Fries, T. G. Huntington, S. M. Dabney, J. M. Sharpe, W. J. Parton, and D. S. Ojima, Dynamic replacement and loss of soil carbon on eroding cropland, *Global Biogeochem. Cycles*, *13*, 885–901, 1999.
- Harrison, K., W. Broecker, and G. Bonani, A strategy for estimating the impact of CO₂ fertilization on soil carbon storage, *Global Biogeochem. Cycles*, *7*, 69–80, 1993.
- Hay, R. K. M., Harvest index: A review of its use in plant breeding and crop physiology, *Annu. Appl. Biol.*, *126*, 197–216, 1995.
- Hillel, D., *Fundamentals of Soil Physics*, 413 pp., Academic, San Diego, Calif., 1980.
- Houghton, R. A., J. L. Hackler, and K. T. Lawrence, The U.S. carbon budget: Contributions from land-use change, *Science*, *285*, 574–578, 1999.
- Howard, D. M., and P. I. A. Howard, Relations between CO₂ evolution, moisture content and temperature for a range of soil types, *Soil Biol. Biochem.*, *25*, 1537–1546, 1993.
- Huddleston, J. S., Soil survey of Tate County, Mississippi, report, USDA Soil Conserv. Serv., Washington, D. C., 1967.
- Huggins, D. R., and D. J. Fuchs, Long-term N management effects on corn yield and soil C of an Aquic Haplustoll in Minnesota, in *Soil Organic Matter in Temperate Agroecosystems: Long-Term Experiments in North America*, edited by E. A. Paul et al., pp. 121–128, CRC Press, Boca Raton, Fla., 1997.

- Huntington, T. G., J. W. Harden, S. M. Dabney, D. A. Marion, C. Alonso, J. M. Sharpe, and T. L. Fries, Soil, environmental, and watershed measurements in support of carbon cycling studies in northwestern Mississippi, *U.S. Geol. Surv. Open File Rep.*, 98-501, 1998.
- Hurt, G. C., S. W. Pacala, P. R. Moorcroft, J. Caspersen, E. Shevliakova, R. A. Houghton, and I. B. Moore, Projecting the future of the U.S. carbon sink, *Proc. Natl. Acad. Sci. U. S. A.*, 99, 1389–1394, 2002.
- Jackson, R. B., J. Canadell, J. R. Ehleringer, H. A. Mooney, O. E. Sala, and E. D. Schulze, A global analysis of root distributions for terrestrial biomes, *Oecologia*, 108, 389–411, 1996.
- Lal, R., Global soil erosion by water and carbon dynamics, in *Soil and Global Change*, edited by R. Lal et al., pp. 131–142, CRC Press, Boca Raton, Fla., 1995.
- Lee, J. L., D. L. Phillips, and R. Liu, The effect of trends in tillage practices on erosion and carbon content of soils in the U.S. corn belt, *Water Air Soil Pollut.*, 70, 389–401, 1993.
- Lee, J. L., D. L. Phillips, and R. F. Dodson, Sensitivity of U.S. corn belt to climate change and elevated CO₂: II. Soil erosion and organic carbon, *Agric. Syst.*, 52, 503–521, 1996.
- Li, C., J. Aber, F. Stange, K. Butterbach-Bahl, and H. Papen, A process-oriented model of N₂O and NO emissions from forest soils: 1. Model development, *J. Geophys. Res.*, 105, 4369–4384, 2000.
- Lin, D. M., and J. W. Doran, Effects of water-filled pore space on carbon dioxide and nitrous oxide production in tilled and non-tilled soils, *Soil Sci. Soc. Am. J.*, 48, 1267–1272, 1984.
- Liu, S., D. S. Schimel, W. A. Reiners, and M. Keller, Simulation of nitrous oxide and nitric oxide emissions from tropical primary forests in the Costa Rican Atlantic Zone, *Environ. Modell. Software*, 15, 727–743, 2000.
- Malhi, S. S., N. M. Izaurralde, and E. D. Solberg, Influence of top soil removal on soil fertility and barley growth, *J. Soil Water Conserv.*, 49, 96–101, 1994.
- Metherell, A. K., L. A. Harding, C. V. Cole, and W. J. Parton, CENTURY Soil Organic Matter Model Environment: Technical Documentation, Agroecosystem Version 4.0, *Tech. Rep. 4*, Great Plains Syst. Res. Unit, Fort Collins, Colo., 1993.
- Mokma, D. L., and M. A. Sietz, Effects of soil erosion on Marlette soils in south-central Michigan, *J. Soil Water Conserv.*, 47, 325–327, 1992.
- Parton, W. J., Predicting soil temperatures in shortgrass steppe, *Soil Sci.*, 138, 93–101, 1984.
- Parton, W. J., D. S. Schimel, C. V. Cole, and D. S. Ojima, Analysis of factors controlling soil organic matter levels in Great Plains grasslands, *Soil Science Soc. Am. J.*, 51, 1173–1179, 1987.
- Parton, W. J., et al., Observations and modeling of biomass and soil organic matter dynamics for the grassland biome worldwide, *Global Biogeochem. Cycles*, 7, 785–809, 1993.
- Paul, E. A., K. Paustian, E. T. Elliot, and C. V. Cole, *Soil Organic Matter in Temperate Agroecosystems: Long-Term Experiments in North America*, 414 pp., CRC Press, Boca Raton, Fla., 1997.
- Peng, C., M. J. Apps, H. Jiang, J. Liu, and Q. Dang, TRIPLEX: A generic hybrid model for predicting forest growth and carbon and nitrogen dynamics, *Ecol. Modell.*, 153, 109–130, 2002.
- Potter, C. S., et al., Terrestrial ecosystem production: a process model based on global satellite and surface data, *Global Biogeochem. Cycles*, 7, 811–841, 1993.
- Renault, P., and J. Sierra, Modeling oxygen diffusion in aggregated soils: II. Anaerobiosis in topsoil layers, *Soil Sci. Soc. Am. J.*, 58, 1023–1030, 1994.
- Renault, P., and P. Stengel, Modeling oxygen diffusion in aggregated soils: I. Anaerobiosis inside the aggregates, *Soil Sci. Soc. Am. J.*, 58, 1017–1023, 1994.
- Riggs, T. J., P. R. Hansen, N. D. Start, D. M. Miles, C. L. Morgan, and M. A. Ford, Comparison of spring barley varieties grown in England and Wales between 1880 and 1980, *J. Agric. Sci. Cambridge*, 97, 599–610, 1981.
- Rooney, J. M., and R. A. Leigh, Dry matter and nitrogen partitioning of the grain of winter wheat (*Triticum aestivum* L.) cultivars grown on Broadbalk since 1843, *Aspects Appl. Biol.*, 34, 219–227, 1993.
- Russel, W. A., Genetic improvements of maize yields, *Adv. Agron.*, 46, 245–298, 1991.
- Schertz, D. L., Effect of past soil erosion on crop production, *J. Soil Water Conserv.*, 44, 604–608, 1989.
- Schimel, D. S., D. C. Coleman, and K. A. Horton, Soil organic matter dynamics in paired rangeland and cropland toposequences in North Dakota, *Geoderma*, 36, 201–214, 1985.
- Schimel, D. S., et al., Climatic, edaphic, and biotic controls over storage and turnover of carbon in soils, *Global Biogeochem. Cycles*, 8, 279–293, 1994.
- Schimel, D. S., I. G. Enting, M. Heimann, T. M. L. Wigley, D. Raynaud, D. Alves, and U. Siegenthaler, CO₂ and the carbon cycle, in *Climate Change 1995*, edited by J. T. Houghton et al., pp. 35–71, Cambridge Univ. Press, New York, 1995.
- Schimel, D. S., et al., Recent patterns and mechanisms of carbon exchange by terrestrial ecosystems, *Nature*, 414, 169–172, 2001.
- Schumacher, T. E., M. J. Lindstrom, D. L. Mokma, and W. W. Nelson, Corn yield: Erosion relationships of representative loess and till soils in the North Central United States, *J. Soil Water Conserv.*, 49, 77–81, 1994.
- Sharpe, J., J. W. Harden, S. Dabney, D. S. Ojima, and W. J. Parton, Implementation of Century ecosystem model for an eroding hillslope in Mississippi, *U.S. Geol. Surv. Open File Rep.*, 98-440, 1998.
- Sharpley, A. N., and J. R. Williams, EPIC-Erosion/Productivity Impact Calculator: 1. Model documentation, *Tech. Bull. 1768*, 235 pp., U.S. Dep. of Agric., Washington, D. C., 1990.
- Sinclair, T. R., Historical changes in harvest index and crop nitrogen accumulation, *Crop Sci.*, 38, 638–644, 1998.
- Skopp, J., M. D. Jawson, and J. W. Doran, Steady-state microbial activity as function of soil water content, *Soil Sci. Soc. Am. J.*, 54, 1619–1625, 1990.
- Slater, C. S., and E. A. Carleton, The effect of erosion on losses of soil organic matter, *Soil Sci. Soc. Am. Proc.*, 3, 123–128, 1938.
- Smith, P., et al., A comparison of the performance of nine soil organic matter models using databases from seven long-term experiments, *Geoderma*, 81, 153–225, 1997.
- Smith, S. V., W. H. Renwick, R. W. Buddenmeier, and C. J. Crossland, Budgets of soil erosion and deposition for sediments and sedimentary organic carbon across the conterminous United States, *Global Biogeochem. Cycles*, 15, 697–707, 2001.
- Stallard, R. F., Terrestrial sedimentation and the carbon cycle: Coupling weathering and erosion to carbon burial, *Global Biogeochem. Cycles*, 12, 231–257, 1998.
- Starr, G. C., R. Lal, R. Malone, D. Hothem, L. Owens, and J. Kimble, Modeling soil carbon transported by water erosion processes, *Land Degrad. Dev.*, 11, 83–91, 2000.
- Tiessen, H. J. W., B. Steward, and J. R. Bettaby, Cultivation effects on the amounts and concentration of carbon, nitrogen, and phosphorus in grassland soils, *Agron. J.*, 74, 831–885, 1982.
- Van Dam, D., E. Veldkamp, and N. van Breemen, Soil organic carbon dynamics: Variability with depth in forested and deforested soils under pasture in Costa Rica, *Biogeochemistry*, 39, 343–375, 1997.
- Van Veen, J. A., and E. A. Paul, Organic carbon dynamics in grassland soils: 1. Background information and computer simulation, *Can. J. Soil Sci.*, 61, 185–201, 1981.
- VEMAP Members, Vegetation/ecosystem modeling and analysis project: Comparing biogeography and biogeochemistry models in a continental-scale study of terrestrial ecosystem responses to climate change and CO₂ doubling, *Global Biogeochem. Cycles*, 9, 407–437, 1995.
- Vermeulen, S. J., P. Woormer, B. M. Campbell, W. Kamukondiwa, M. J. Swift, P. G. H. Frost, C. Chivaura, H. K. Murwira, F. Mutambanengwe, and P. Nyathi, Use of the SCUAF model to simulate natural miombo woodland and maize monoculture ecosystems in Zimbabwe, *Agrifor. Ecosyst.*, 22, 259–271, 1993.
- Voldeng, H. D., E. R. Cober, D. J. Hume, C. Gillard, and M. J. Morrison, Fifty-eight years of genetic improvement of short-season soybean cultivars in Canada, *Crop Sci.*, 37, 428–432, 1997.
- Voroney, R. P., J. A. Van Veen, and E. A. Paul, Organic C dynamics in grassland soils: 2. Model validation and simulation of the long-term effects of cultivation and rainfall erosion, *Can. J. Soil Sci.*, 61, 211–224, 1981.
- Webber, L. R., Soil physical properties and erosion control, *J. Soil Water Conserv.*, 19, 28–30, 1964.
- Williams, J. R., The EPIC Model, in *Computer Models of Watershed*, edited by V. P. Singh and J. R. Williams, pp. 909–1000, Water Resour., Highlands Ranch, Colo., 1995.
- Wofsy, S. C., et al., Net exchange of CO₂ in a mid-latitude forest, *Science*, 260, 1314–1317, 1993.
- Wych, R. D., and D. C. Rasmusson, Genetic improvement in malting barley cultivars since 1920, *Crop Sci.*, 23, 1037–1040, 1983.
- Yin, X., and P. A. Arp, Predicting forest soil temperatures from monthly air temperature and precipitation records, *Can. J. For. Res.*, 23, 2521–2536, 1993.

T. G. Huntington, U.S. Geological Survey, 196 Whitten Rd., Augusta, ME 04330, USA. (thunting@usgs.gov)

S. Liu and N. Bliss, U.S. Geological Survey, Earth Resources Systems Observation Data Center, SAIC, Sioux Falls, SD 57198, USA. (sliu@usgs.gov; bliss@usgs.gov)

E. Sundquist, U.S. Geological Survey, 384 Woods Hole Road, Woods Hole, MA 02543, USA. (esundqui@usgs.gov)